GA–A25128

CORROSION SCREENING OF CONSTRUCTION MATERIALS FOR HYDROGEN IODIDE DECOMPOSITION HEAT EXCHANGER FABRICATION

Milestone Completion Report (January 2004 through June 2005)

by

B. WONG, L.C. BROWN, and G.E. BESENBRUCH

DATE PUBLISHED: JULY 2005

GENERAL ATOMICS

DISCLAIMER

GA–A25128

CORROSION SCREENING OF CONSTRUCTION MATERIALS FOR HYDROGEN IODIDE DECOMPOSITION HEAT EXCHANGER FABRICATION

Milestone Completion Report (January 2004 through June 2005)

by

B. WONG, L.C. BROWN, and G.E. BESENBRUCH

Prepared under
Research Foundation Contract No. RF-05-HTHX-005
for University of Nevada-Las Vegas

GENERAL ATOMICS PROJECT 30231
DATE PUBLISHED: JULY 2005

GENERAL ATOMICS

EXECUTIVE SUMMARY

The scaling up of the Sulfur-Iodine (S-I) cycle and its realization at an industrial level depends to a large extend on finding the right materials of construction. The material challenges are substantial because of the combination of corrosive chemicals operating at elevated temperatures. A plan, which includes *screening*, *development* and *prototyping* phases, has been established to identify the appropriate construction material candidates. This will also institute a database for materials data which is agonizingly lacking.

This report presents the result of material screening tests that have been conducted at General Atomics (GA) to identify heat exchanger construction material for HI decomposition (Sec. 3 of the S-I cycle). Corrosion coupon immersion tests were used to determine the corrosion resistance and applicability of various materials in HI_x (HI + H_2O + H_2) at temperatures up to 310°C. A materials survey was conducted to form the list of candidates. A total of 23 different candidates selected from 5 classes of materials, refractory metals, reactive metals, superalloys, ceramics and graphite, were tested in HI_x at the reactive column feed and boiler conditions for 100 hours or more. Material corrosion performance is based on the samples' post test weight change and physical attribute. Detailed characterization of specimens is being carried out at the University of Nevada, Las Vegas.

A corrosion testing facility for HI decomposition was built at General Atomics for this work and high temperature, high pressure corrosion coupon immersion test systems were designed and constructed. The systems are able to conduct corrosion tests without incident thus verifying the design.

All the metallic specimens tested exhibit color change. This is due to the growth of a passivation layer on the coupons which arises from the reaction between the coupons and HI_x. The metal coupons that are corrosion resistant against HI_x all developed an uniform passivation whereas corroded coupons all show uneven color distribution. Corrosion test results have shown that Ta, Nb and their alloys, SiC, some Si-SiC ceramic composites and mullite all possess excellent corrosion resistance against HI_x under the reaction conditions. On the other hand, recognized corrosion resistant materials such as Zr, Mo, C-276 (Ni-based), Haynes 188 (Co-based) and alumina all exhibit weight loss and corrode readily. The corrosion observed is in the form of either pitting and/or material dissolution. Extruded graphite was found to absorb a substantial amount of HI_x during test but did not show any sign of corrosion. Characterization of specimen is ongoing at UNLV in an effort to understand the corrosion mechanism.

The corrosion rate of the materials tested in HI_x has been calculated and it was found that the test temperature has the largest effect on corrosion rate. Based on the result, we have selected three candidates, Ta-2.5W, Ta-10W and Nb-10Hf, for developmental testing. This includes long term immersion coupon testing and studying the effect of material processing on crack initiation and growth in these materials.

The overall objective of this phase of the program has been met:

- A plan to identify the materials of construction for HI decomposition has been put in place.
- Two immersion corrosion test systems that are able to accommodate coupons and larger specimens have been constructed and are in operation.
- A total of 23 materials, based on the results of a material survey, have been screened. A database on the corrosion performance and rate of various materials in HI_x has been established.
- Three materials candidates, Ta-2.5W, Ta-10W and Nb-10Hf have been identified for developmental testing based on their corrosion performance and availability.

The screening result shows that even though the challenges are hard, there are materials that are capable of handling the HI_x environment. The developmental phase will identify the appropriate manufacturing techniques that can best fabricate the heat exchangers prototypes from these materials.

TABLE OF CONTENTS

TABLE OF CONTENTS (Continued)

LIST OF FIGURES

LIST OF FIGURES (Continued)

LIST OF TABLES

LIST OF TABLES (Continued)

1. INTRODUCTION

1.1. S-I CYCLE

The Sulfur Iodine (SI) water splitting cycle for hydrogen (H_2) production offers a promising approach to high efficiency production of H_2 using nuclear power (Fig. 1). The cycle consists of three coupled sections:

- *Section 1 – Sulfuric Acid and Hydriodic Acid Generation (Bunsen Reaction)*. This section receives recycled sulfur dioxide (SO_2) gas from Sec. 2 and iodine (I_2) from Sec. 1 and employs the Bunsen reaction (1) to form two immiscible liquid phases. The upper phase is sulfuric acid (H_2SO_4) and the lower phase is a mixture of HI, H_2O and I_2 (HI_x). The two phases are sent to the two other sections to be decomposed separately.

$$SO_2(g) + I_2(l) + H_2O(g) \rightarrow HI(l) + H_2SO_4(l) \rightarrow 120°C. \quad (1)$$

- *Section 2 – Sulfuric Acid Concentration and Decomposition*. This section concentrates the H_2SO_4 received from Section 1 and then decomposes it into SO_2, O_2 and H_2O at high temperature. The decomposed products are returned to Sec. 1.

$$H_2SO_4(g) \rightarrow H_2O(g) + SO_2(g) + \rightarrow O_2(g) \rightarrow 900°C \quad . \quad (2)$$

- *Section 3 – Hydrogen Iodide Decomposition*. This section receives HI_x from Sec. 1. Hydrogen Iodide (HI) is distilled from HI_x before it can be decomposed into H_2 and I_2. The recycled I_2 is returned to Sec. 1.

$$HI(g) \rightarrow H_2(g) + I_2(g) \rightarrow 450°C \quad . \quad (3)$$

The cycle has no effluent and all the chemicals are recycled. The only required inputs are heat and water. The baseline design for the current SI work is the system configuration described in "High Efficiency Generation of Hydrogen Fuels Using Nuclear Power," General Atomics Report GA-A24285 [1].

Due to the high reaction temperature and chemicals involved, the reaction environment within the cycle is extremely corrosive and poses substantial material challenges. In order to realize a stable, safe and functional H_2 production plant, careful selection of materials, fabrication techniques and designs to manufacture the heat exchangers, reaction chambers and other components must be taken.

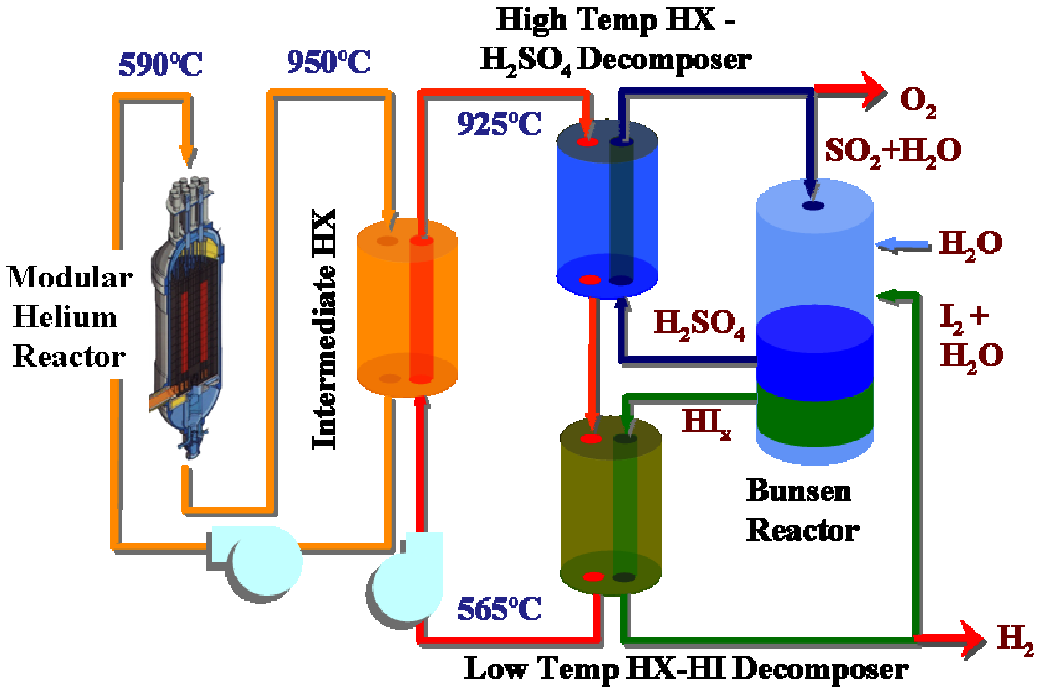

Fig. 1. The Nuclear SI Hydrogen Production Cycle.

General Atomics (GA) is leading the project to identify material(s) suitable for HI decomposition heat exchanger construction. This work is undertaken in collaboration with the University of Nevada at Las Vegas (UNLV). Sandia National Laboratory (SNL) and Commissariat à l'Énergie Atomique (CEA) are identifying materials suitable for Sulfuric Acid Decomposition and the Bunsen Reaction respectively.

1.2. HI DECOMPOSITION

Section 3, HI decomposition, receives the reaction product HI_x ($HI + I_2 + H_2O$) from the Bunsen section in liquid form for processing. HI must first be distilled from HI_x before it can be decomposed into $H_2 + I_2$. There are two avenues to carry out this distillation-decomposition process. They are *Reactive Distillation* and *Extractive Distillation*. The reaction conditions and the chemicals involved are different between them.

1.2.1. Reactive Distillation

In reactive distillation, HI is distilled from HI_x through boiling. The equilibrium vapor pressure at 300°C, the desired temperature for HI decomposition is about 50 bar (~750 psi). Figure 2 shows a schematic of the reactive distillation flow sheet. The HI_x from the Bunsen section is heated to 262°C from 120°C and is then fed into the reactive

column. At the bottom of the column, HI_x is boiling at 310°C. The HI, I_2 and H_2O vapor flow through a bed of catalyst at the top half of the column and HI is spontaneously decomposed into H_2 and I_2 gases. A condenser at the top of the column condenses any un-reacted HI and I_2 and H_2O. The I_2 is fed back into Sec. 1 for the Bunsen reaction and H_2 is bled off as a compressed gas for storage or use. The process has been modeled [2] and is currently being experimentally verified.

1.2.2. Extractive Distillation

Extractive distillation utilizes concentrated phosphorus acid (H_3PO_4) to extract HI and H_2O from HI_x as they, unlike I_2, are soluble in H_3PO_4. HI is then distilled off and decomposed [3]. A schematic of the process flow sheet is shown in Fig. 3. Concentrated phosphoric acid (up to 95%) is added to HI_x feed from the Bunsen Reaction at 120°C to form a two phase liquid mixture of I_2 and HI + H_2O + H_3PO_4 [Fig. 3(a)]. The separated I_2 is returned back to Sec. 1 for the Bunsen section. HI gas is distilled from boiling HI + H_2O + H_3PO_4 and send to the reactive column for decomposition [Fig. 3(b)]. The phosphoric acid (H_3PO_4 + H_2O) is then concentrated through a series of boilers and added to the incoming HI_x feed to anew the process.

1.3. IDENTIFICATION OF CONSTRUCTION MATERIALS FOR HI DECOMPOSITION

A plan to identify the material of construction for the S-I cycle heat exchangers has been established. A detailed description can be found in the GA-SNL joint report titled *"Engineering Materials Requirements Assessment for the SI Thermochemical Cycle"* [4]. The plan to select materials for HI decomposition is divided into three stages: *screening*, *development* and *prototype* (Fig. 4). In the first stage, corrosion coupon immersion tests were conducted using the most corrosive reaction conditions to screen a list of containment material candidates. The development stage takes a more comprehensive look at different aspects of the qualified materials' performance and applicability. The study will include:

- Long term corrosion effect of the reaction environment on materials,
- Processing effects on the corrosion properties of the material candidate,
- The capacity to manufacture components from the selected materials.

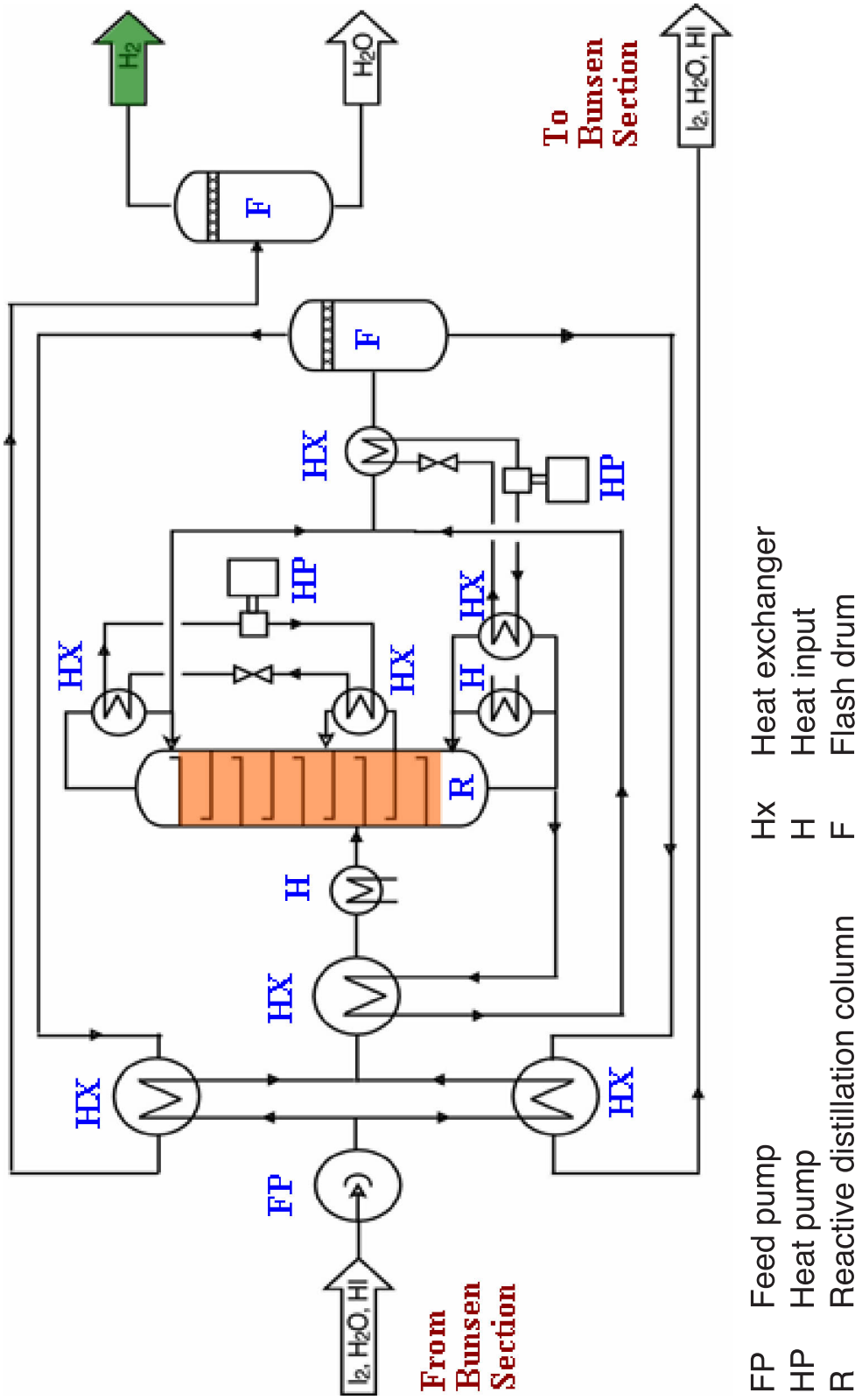

Fig. 2. HI reactive distillation and decomposition flowsheet.

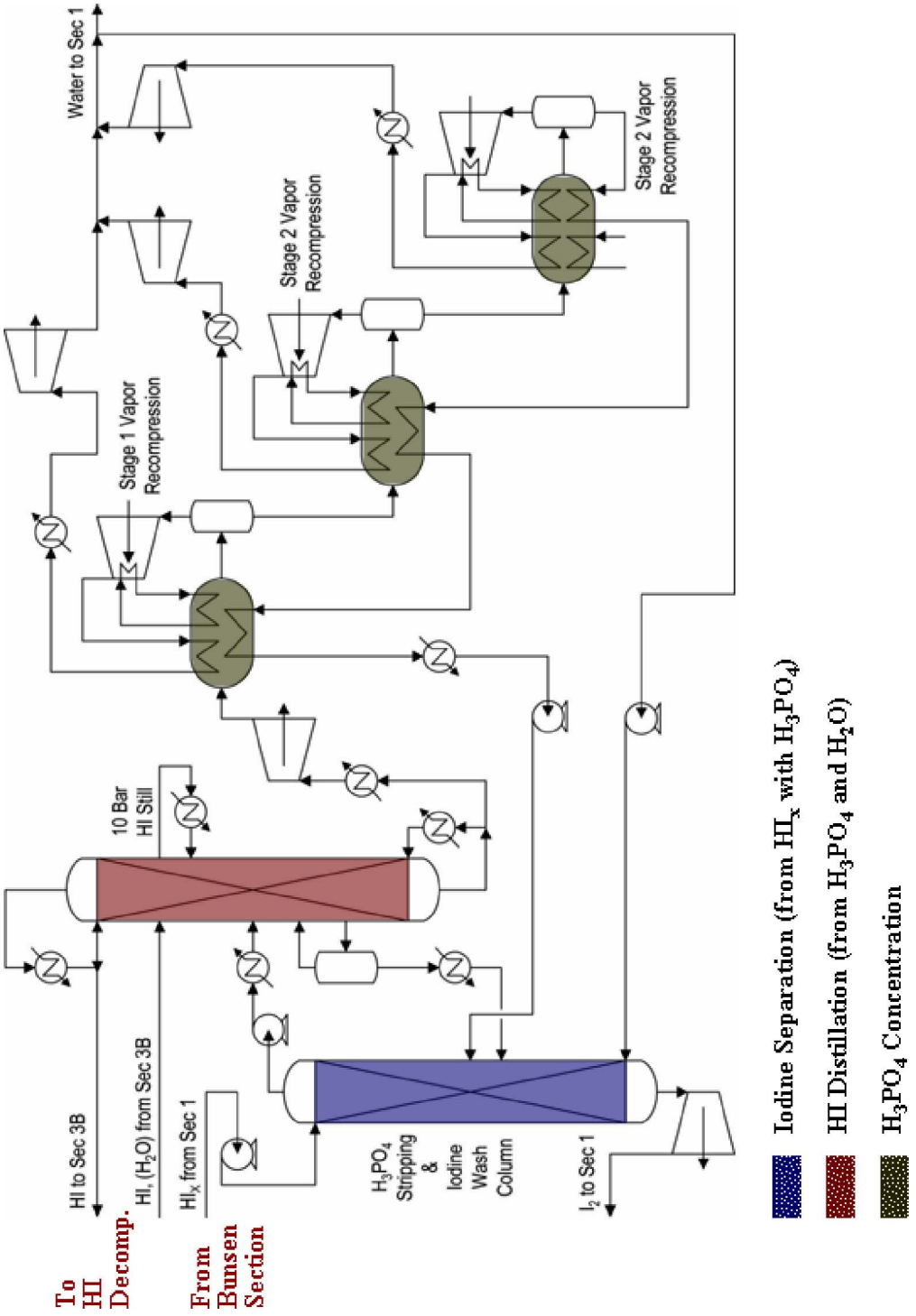

Fig. 3. (a) HI extractive distillation flowsheet — iodine extraction and HI distillation.

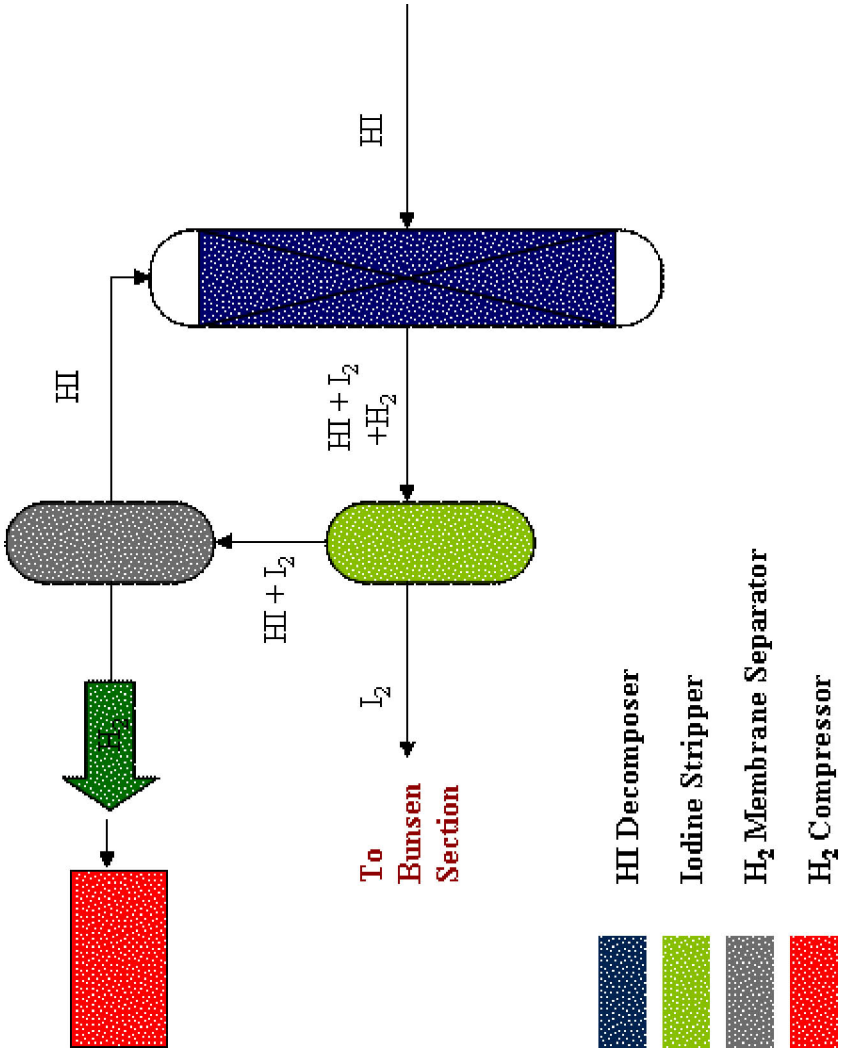

Fig. 3. (b) HI extractive distillation flowsheet — HI decomposition.

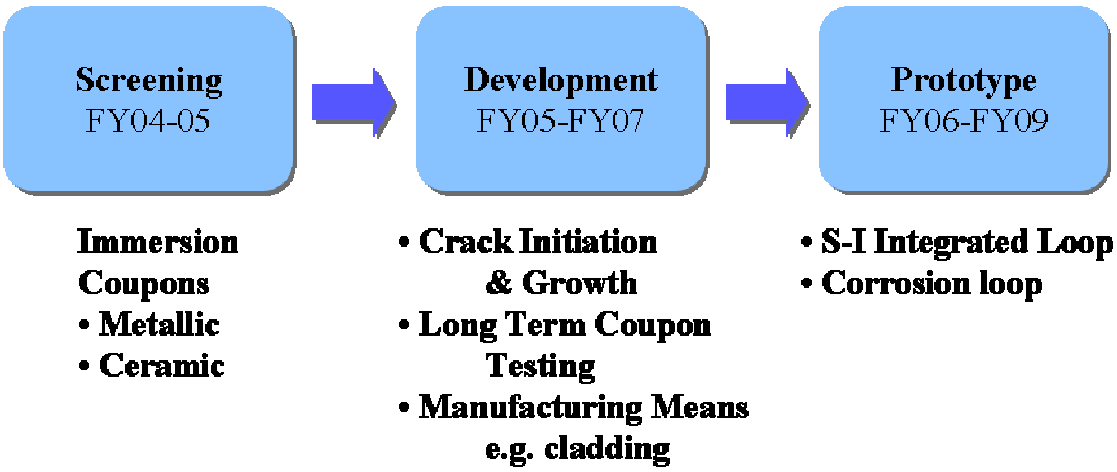

Fig. 4. Plan to identify construction material for HI decomposition heat exchanger.

In the final phase of this program, prototype components built from qualified construction materials will be tested in a corrosion loop with cycling chemicals. This provides an opportunity to assess the long term performance of manufactured components and evaluate new fabrication and design techniques such as cladding and lining.

This report summarizes the immersion coupon corrosion test results and qualifies a list of candidates that will undergo further developmental testing.

2. MATERIALS SURVEY

In reactive distillation, the corrosive environment is generated by liquid HI_x at various composition and temperatures. On the other hand, a number of chemical mixtures at lower temperature e.g. HI_x(l), conc. H_3PO_4(l), H_3PO_4(l).+ HI_x(l) and HI + I_2 + H_2(l/g) etc. are found within the extractive distillation loop. The reactive distillation environment is deemed more corrosive because of the higher reaction temperature and the process fluids are in liquid form. Liquid medium can accelerate corrosion as ion transport is enhanced in a liquid/aqueous environment. Among all the chemicals associated with HI decomposition, I_2 has the highest capacity to corrode followed by HI and H_3PO_4. The existence of H_2 may also lead to embrittlement issues. It is possible to select materials that are resistant to all the individual chemical. However, combination of chemicals can often create corrosive environment that can not be predicted based on the effect of a single component. A materials survey has been conducted to identify a list of potential materials that can withstand the chemical environment of both reactive and extractive distillation. The survey includes corrosion data for not only HI_x but other aggressive chemicals such as HI, I_2 and H_3PO_4.

2.1. MATERIALS FOR HI_x

Corrosion data of materials in HI_x is extremely limited. The most comprehensive set is from Trester et al. [5]. Table I lists a summary of the immersion coupon test results from their work. The test temperature is applicable to that used in extractive distillation but is about 100°-200°C lower than that required by reactive distillation. Based on this data, refractory metals (Ta, Nb, Mo), reactive metals (Zr), ceramics (SiC) and carbon based materials have the best prospect of being compatible with HI_x at high temperature.

Ceramic materials such as Al_2O_3 have also been shown to work well in the presence of I_2 but their application in traditional heat exchanger design is limited as they have very low thermal conductivity. On the other hand, recent modeling results from micro-channel heat exchanger indicated that there may be an advantage in using low thermal conductivity material in those designs.

Table I
GA Results (1977-1981) Summary from Trester and Staley [5]

Test	HI (%)	I_2 (%)	H_2O (%)	Temp. (°C)	Pres.	Time (Hour)	Materials Tested		
							Excellent	Fair	Poor
1	20* (4)†	20 (2)	60 (93)	22	atm	8760	Mo, Nb-1%Zr, Ta, Ta-10%W, Ti(as cast), Ti-0.5%Pd, Zr, Zircaloy2 TFE, FEP, Kalrez 1050, Kel-F 3700, Fluorel 2174, Viton A, Parker V-834-70	Chlorimet 2 & 3, Hastelloy B2 and C276 PVC, Polycarbonate, Vespel Sp.1, CPE, FETFE	Inconel 600, Monel, Haynes, Hastelloy G, 304 Stainless Nylon, Mylar, Silicone
2	30 (15)	50 (13)	20 (72)	200-450	13.1–17.2 MPa	5–10	Mo, Ta	Ti	Inconel 600
3	11 (11)	82 (40)	7 (49)	97	atm	3170	Mo, Nb-1%Zr, Ta, Zr TFE, FEP, PFA, Tefzel (Teflon) SiC, Alumina, Boronsilicate glass	Ti–0.2%Pd(anodized), Hastelloy B2, Durichlor 51, Zircaloy2, Zr702 Kynar 450 Zirconia	Duriron D, Chlorimet 2, C276, Ti-0.5%Pd, Gold, Platinum CPVC, Polypropylene
4	11 (11)	82 (40)	7 (49)	125	atm	500	Mo, Nb, Nb-1%Zr, Ta Alumina, vitreous carbon	TFE, FEP, PFA	Lead Viton VTX 5362, Viton B, Carbonrundum
5‡	24 (12)	55 (14)	21 (74)	134	atm	0.178	Mo, Nb, Nb-1%Zr, Ta, Zircaloy2, Ta-10%W, Zr	Ti–0.5%Pd	Ti-0.2%Fe-0.25%O (annodized Ti)

*wt%, †molar%, ‡circulating HI_X.
Ni based alloys: Hastelloy, Chlorimet, Inconel and Monel; Iron based alloys: Duriron, Durichlor; Cobalt based alloys: Haynes Summary

2.2. MATERIALS FOR IODINE

I_2 is one of the most corrosive chemicals. Table II lists the corrosion rate of a number of common corrosion resistant materials in I_2 at 300° and 450°C, respectively [6]. Although the data shows that noble metals are stable in an I_2 environment, they have been found to dissolve in HI_x due to the addition of HI acid (Table I). Refractory metals are the next best group of materials to be used with I_2.

Table II
Corrosion Rate of Alloy in Pure Iodine at High Temperature

	Corrosion Rate (mils/yr)	
Alloy	**300°C**	**450°C**
Platinum	0	0.0055
Tungsten	0	0.008
Gold	0	0.024
Molybdenum	0.003	0.033
Tantalum	0.004	0.88
Alloy B	0.057	0.46
Alloy 600	0.107	0.54

2.3. MATERIALS FOR HI ACID

HI is a strong reducing acid. Although it is a common reagent in organic chemistry, corrosion data of materials in HI at evaluated temperature is limited. Table III lists a summary of the available data [7]. Niobium and other refractory metals are good construction materials candidates.

Table III
Corrosion Rate of Alloy in HI Acid

Alloy	**Temperature (°C)**	**Corrosion Rate (mils/yr)**	**Comments**
Titanium	23	0.15	Conc. 57%
Niobium	<100	0	For all conc.
Gold	25	<0.05	Dilute
Palladium	25	65.7	
Zr702	127	<0.05	Conc. 57wt%

2.4. MATERIALS FOR PHOSPHORIC ACID

Phosphoric acid is commonly used in chemical industry and can generally be handled with high Mo grade stainless steel such as alloy 28 and G-30. Ni-Mo alloys have also been used with phosphoric acid (Table IV) [8]. At high concentration and boiling temperature, Ta, Nb and their alloys are good candidates for materials of construction. Table V shows the corrosion rate of Ta and Nb alloys in 80% conc. H_3PO_4 at 150 and 200°C respectively [9].

Table IV
Corrosion Rate of Alloys in H_3PO_4

Alloy	Concentration	Temperature (°C)	Corrosion Rate (mils/yr)
316 stainless	85	115	0.144
Hastelloy C	85	Boiling	1.14
Durimet 20	75-85	115	0.233
Haynes 556	85	Boiling	0.84
Inconel 617	85	Boiling	0.66
Monel 400	85	124	0.254
Tantalum	85	100	nil
Niobium	85	100	0.125
Silver	85	140	0.048

Table V
Corrosion Rate of Ta and Nb Alloys in 80% conc. H_3PO_4 at 150°C and 200°C

	Corrosion Rate (mils/yr)	
Alloy	**150°C**	**200°C**
Niobium	59.06	NA
Nb-20Ta	11.81	NA
Nb-40Ta	8.66	492.13
Nb-60Ta	2.76	82.68
Nb-80Ta	0.39	29.92
Tantalum	0.05	5.31

2.5. MATERIALS REQUIREMENTS

The general guidelines to selecting heat exchanger construction materials suitable for HI decomposition can be summarized as follows:

- Selected materials must be corrosive resistant to the working environment.
- The materials must have good thermal conductivity to be used for heat exchanger application.
- Components manufactured from the materials must have suitable mechanical properties and can be designed with time independent data.
- The materials must have good hot and cold formability, weldability, and availability to make building of a hydrogen production plant practical.
- The possibility for non-destructive testing while the components are being fabricated and while they are in service.

3. EXPERIMENTAL TEST PLAN

3.1. TEST CONDITIONS

Since the reactive distillation environment is more corrosive, it is employed as the baseline environment for corrosion testing. Materials which perform well in HI_x should be applicable to the extractive process as the chemicals are similar but at lower temperatures. Analysis of the HI reactive distillation reaction flow sheet revealed two locations that are deemed most corrosive with respect to heat transfer within the section. They are the reactive column feed and the column boiler respectively. The chemical composition and physical condition at these points are listed in Table VI and they will be referred to as the feed and boiler condition hereafter.

Coupons made from different materials are submerged in HI_x at the conditions stated above for up to 120 hours. According to flowsheet calculations, the HI_x equilibrium vapor pressure is around 50 bar at boiling. In order to suppress vapor formation, the test is conducted at a pressure in excess of 100 bar at the reaction temperature so HI_x remains in liquid form.

Table VI
Corrosion Coupon Immersion Test Conditions

	Temperature	Mole Fraction (*Weight Fraction*)		
Column Reactants	**(°C)**	**HI**	**I_2**	**H_2O**
1. Feed HI_x	262	0.10 (*0.084*)	0.38 (*0.813*)	0.52 (*0.079*)
2. Column Boiler	310	0.02 (*0.062*)	0.89 (*0.982*)	0.09 (*0.007*)

3.2. MATERIAL CANDIDATES

A list of potential candidates from different group of materials has been assembled based on the materials survey results and they are listed in Table VII. Five categories of materials will be tested including refractory and reactive metals, superalloys, ceramics and graphite. The coupons are in general 1 in. x 2 in. x 0.125 in. in dimension. However, other shapes are used if the materials are not available in sheet form.

Table VII
List of Materials Chosen for Testing in the HI_x Corrosion Coupon Immersion Test

	Materials
Refractory metals	• Ta, Ta-2.5%W, Ta-10%W, Ta-40%Nb • Nb, Nb-1%Zr, Nb-7.5%Ta, Nb-10%Hf • Mo, Mo-47Re
Reactive metals	• Zr702, Zr 705
Superalloy	• C-276 (Ni-based), Haynes 188 (Co-based)
Ceramics	• Sintered SiC, CVD SiC, • Bioker 29 Si-SiC, Splint Si-SiC, Fiber Si-SiC • Alumina, Mullite
Others	• Graphite

3.3. SYSTEM SET UP

A cross section schematic of the high temperature and high-pressure test apparatus is shown in Fig. 5. The system consists of a Blue M 3 zone clamshell tube furnace holding a tubular pressure vessel in which the test cell is placed. It is described in more details in the following sections. Two test systems have been constructed. The smaller system has a pressure vessel with a 2 in. ID whereas the larger on has a vessel ID of 3.5 in. The second system can accommodate specimens which are larger than coupons.

3.3.1. Pressure Vessel

The body of the high-pressure reactor vessels are made from 304 stainless steel and the end caps are made from 316 stainless. They were manufactured by High Pressure Equipment Company, Model TOC15-40 and TOC29-40. The vessels are sealed with 316 stainless steel gaskets for high temperature operation. The maximum room-temperature working pressure of both vessels is 5000 psig (345 bar) and they are rated at 4000 psig (276 bar) at 427ºC. Figure 6 shows a picture of the vessel-furnace set up. Since 304 and 316 stainless are not very resistant to HI and I_2 attack, it is imperative that the contact between the chemicals and the vessel be minimized. This is accomplished by conducting the experiment at a pressure much higher than that of the HI_x equilibrium vapor pressure.

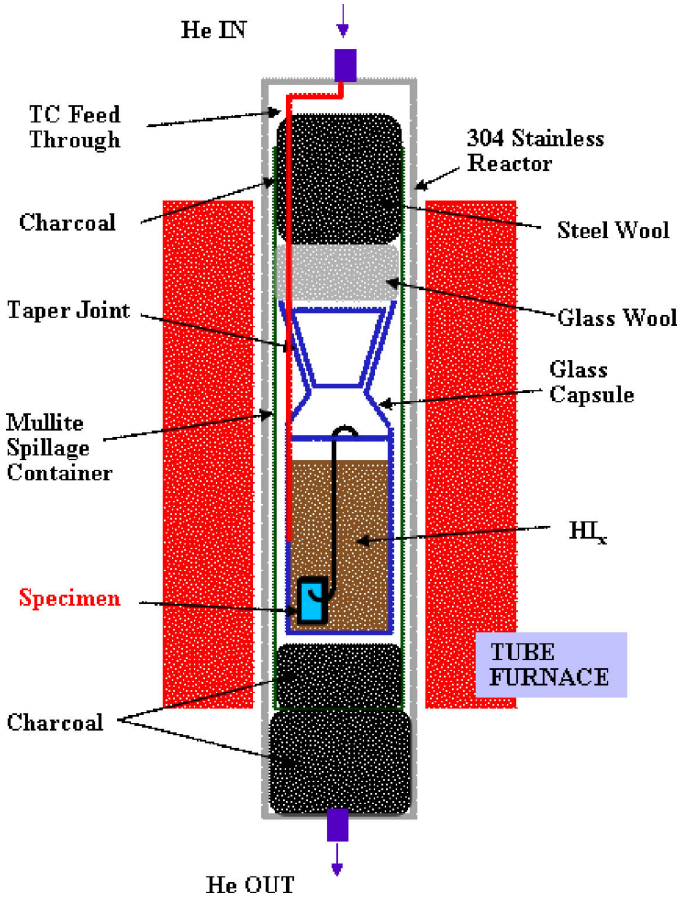

Fig. 5. A cross section schematic of the immersion coupon corrosion test apparatus.

Fig. 6. Test apparatus set up with the pressure vessel tube sitting inside the tube furnace.

3.3.2. Test Cell

The test cell consists of a boronsilicate glass capsule that holds both the coupon and the HI_x [Fig. 7(a)]. Boronsilicate glass has been shown to be extremely inert in HI_x at the present test temperatures. The test coupon hangs freely on a glass rod inside the capsule [Figs 7(b,c)]. The capsule is closed at the top with an end cap using a tapered ground glass joint. A piece of glass wool is place at the top of the capsule to reduce HI_x evaporation.

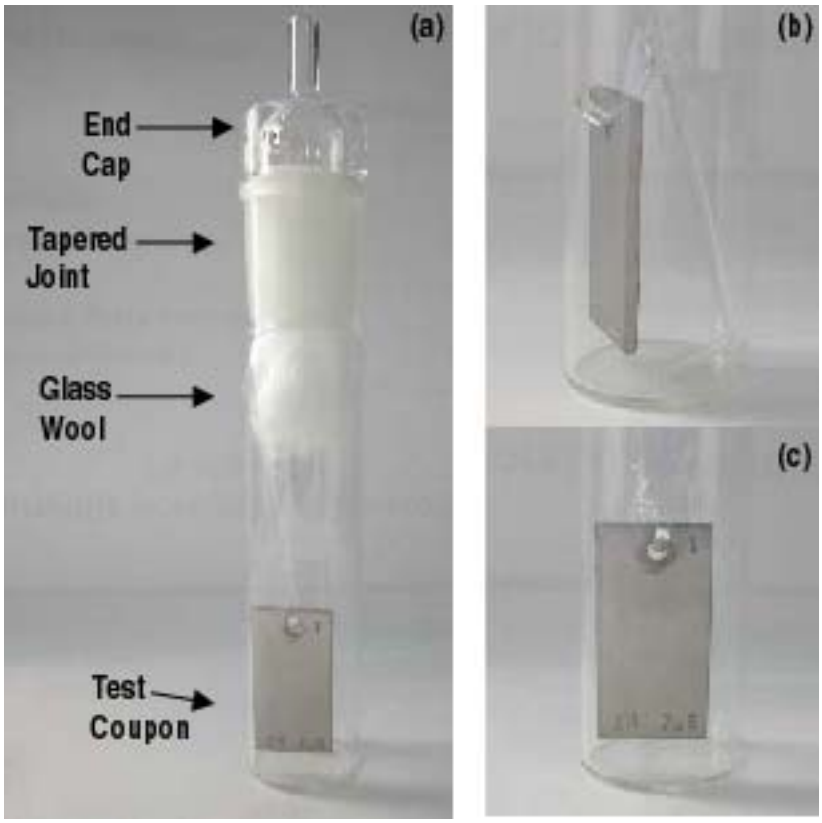

Fig. 7. (a) Test cell setup. (b) and (c) freehanging test coupon.

The total capsule volume is about 180 cc and 60 cc of HI_x is placed inside the capsule to cover the coupon during test. The HI_x is prepared by mixing solid I_2, 57wt% HI acid and H_2O (if necessary) at room temperature. The test medium volume and the amount of chemicals required are calculated based on a solid I_2 density of 4.93 g/cc. Since the liquid density of I_2 is 3.96 g/cc, the actual volume of HI_x should be between 80–95 cc respectively for the two test conditions. This will ensure the entire specimen is submerged during the experiment, even with a small amount of HI_x escaping. A dual chamber design with a glass divider has also been employed to successfully test two specimens simultaneously (Fig. 8). For specimens such as SiC that are too brittle to be

drilled, special specimen holder has been design to keep the coupon in place during test [Fig. 8(c)]. Since the density of SiC is less than HI_x, a weight is attached to the top of the holder to push the specimen down.

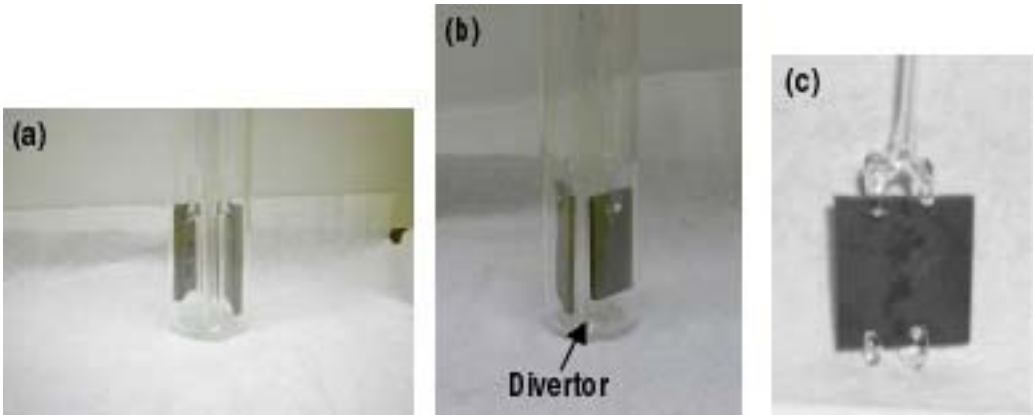

Fig. 8. (a) and (b) Dual chamber glass capsule. (c) Specimen holder for brittle ceramic specimens.

The capsule is placed inside a single closed end mullite tube (Fig. 9) on top of a bed of activated charcoal. The mullite tube provides spillage containment in case the capsule breaks during the experiment and the activated charcoal acts to absorb HI and I_2 during such an event. The open end of the mullite tube is filled with glass and steel wool and charcoal to trap and absorb any vapor that leaks out of the capsule.

The mullite tube is placed inside the pressure vessel and sits on top of a basket of activated charcoal. This charcoal basket is located below the high temperature zone. The cooler temperature improves the charcoal's efficiency to absorb HI and I_2. The free space inside the vessel is filled with steel wool to catch and react with any HI_x vapor. This cuts down the reaction between the vapor with the vessel wall. In the larger test system, a thermal couple is placed next to the glass capsule to provide instant temperature feedback.

Fig. 9. Mullite tube in which the test cell is located.

3.3.3. Test System

A schematic of the piping scheme for the test system is shown in Fig. 10(a). External cold charcoal traps are connected to ends of the pressure vessel to capture any HI and I_2 vapor to ensure the integrity of the external components. A rupture disk and a pressure relief valve are placed in parallel as safety relief in the event of an over pressurized vessel. The two quarter-turn turn valves that control the pressurization of the system are located outside the test enclosure [Fig. 10(b)].

3.4. TEST FACILITIES

The test system is located inside a stainless steel enclosure with a Lexan door to stop any projectile if a rupture occurs (Fig. 11). The enclosure is connected to a blower that vents the volume of the hood. A charcoal filter is mounted in the exhaust line to absorb any released HI or I_2 vapor.

The set up of the test cell and retrieval of the specimen are carried out inside a fume hood next to the enclosure. This prevents the test lab from being contaminated with HI and I_2. The fume hood is vented through a bank of charcoal filter at the blower for HI and I_2 absorption.

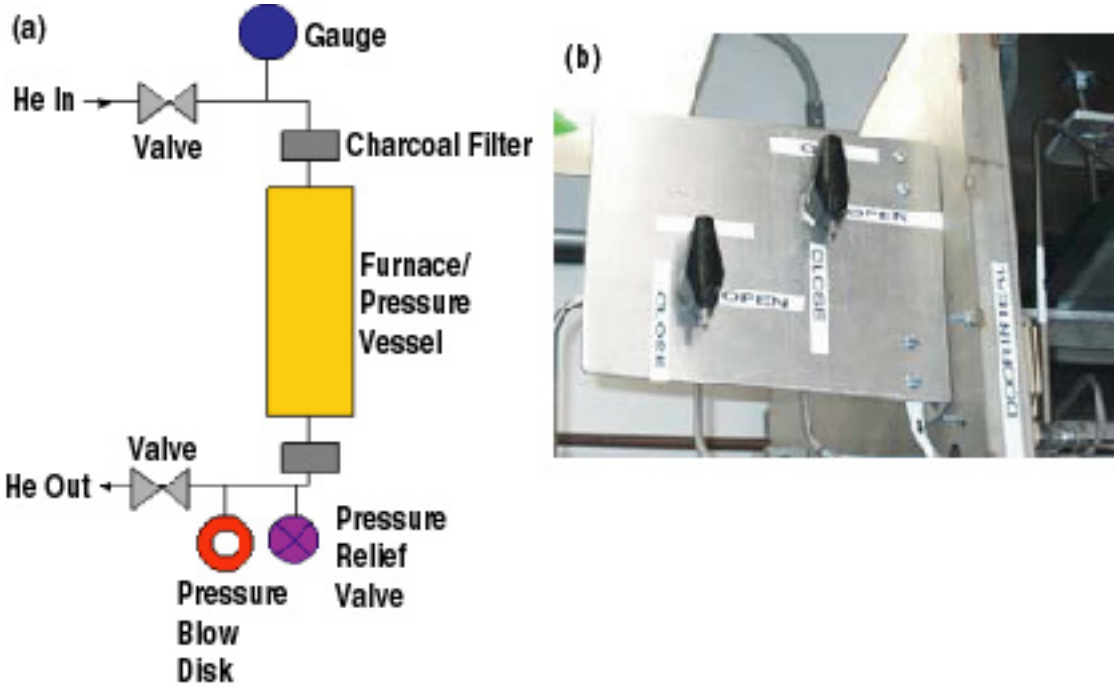

Fig. 10. (a) Piping scheme for the test apparatus set up. (b) Inlet and outlet valves locating outside the test enclosure.

Fig. 11. Immersion corrosion test system enclosure and fume hood.

3.5. OPERATION PROCEDURES

The test cell is assembled inside the fume hood and then transferred to the pressure vessel inside the mullite tube. To reach 100 bar (1470 psi) at the test temperature, the vessel must be pressurized with helium (He) gas to approximately 68 bar (1100 psi) at room temperature. Helium is used to first flush the system and then pressurize the vessel at a rate of 50 psig/5 min until it reaches 1100 psi. The gradual increase in pressure allowed for equalization between the capsule and the vessel through the tapered joint. A leak check is performed on the vessel during this pressurization stage. When the pressure reaches 1100 psi, the valve is closed and the furnace is turned on. The pressure within the vessel increases to the target values of around 1350-1450 psi as the temperature rises to 260^{o} or 310^{o}C.

At the end of each run, the furnace and pressure vessel was cooled down to room temperature by flowing compress air over the top of the pressure vessel. This process takes about 60 minutes. Once the cool down cycle is complete, the outlet valve is opened to relieve the pressure within the pressure vessel. The specimen is then retrieved from the test cell for cleaning and characterization. The test medium was disposed as hazardous waste.

4. RESULTS AND DISCUSSION

4.1. OVERALL SYSTEM FUNCTIONALITY

A total of 52 immersion corrosion coupon tests were conducted. No accident or inadvertent HI_x release occurred. The pressure vessel remained clean and free of corrosion, which indicated that reaction between HI_x vapor and the vessel wall was minimal. Figure 12 shows the test cell before and after a test. The liquid level inside the capsule remains similar which shows that the loss of HI_x due to vaporization is minimal.

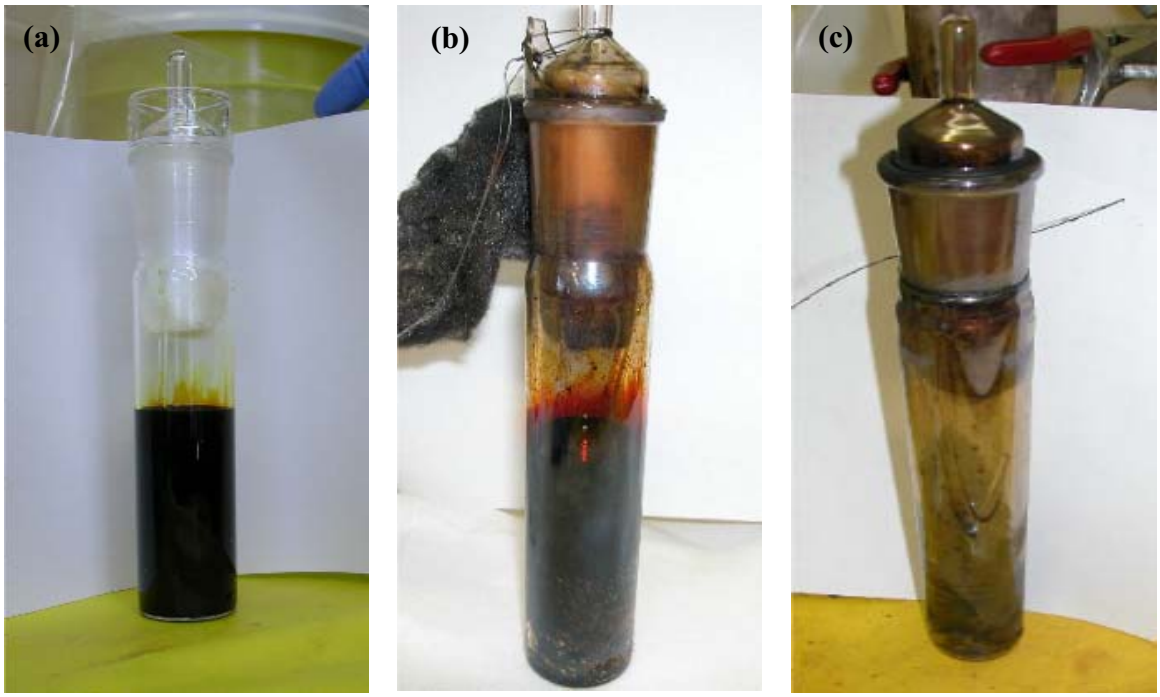

Fig. 12. Test cell: before and after test. (a) Feed composition before test. (b) Feed and (c) boiler composition after test.

Figure 13 shows a coupon embedded in solid I_2 after a test. The weight of the solid is 6% less than the pretest combined weight of I_2, specimen and glass rod. Taking into account the amount loss due to handling, attachment to the capsule and the steel wool, probably only a very minor portion of I_2 or HI evaporated. Hence, the immersion coupon corrosion test system performed as designed with the high pressure suppressing vapor formation.

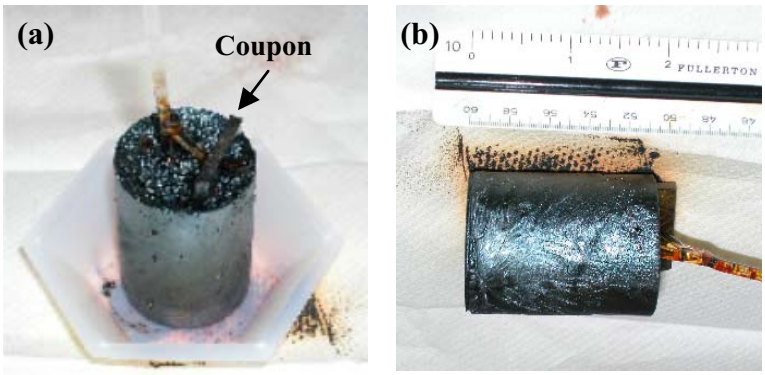

Fi.g. 13. Test coupon embedded in solid I_2 after test.

4.2. SPECIMEN RETRIEVAL

At the completion of each experiment, liquid HI_x phase separates back into solid I_2 and an aqueous HI_x phase upon cooling (Fig. 14). Hence, the coupon is always embedded in the solid I_2 (also Fig, 13). To retrieve the specimen, I_2 is dissolved away using a mixture of alcohol and acetone in an ultrasound bath inside the fume hood. It can take up to three days to dissolve away the I_2. Alternately, one can crack the capsule to retrieve the solid piece of I_2 (Fig. 13) which can be easily be cracked open for specimen retrieval.

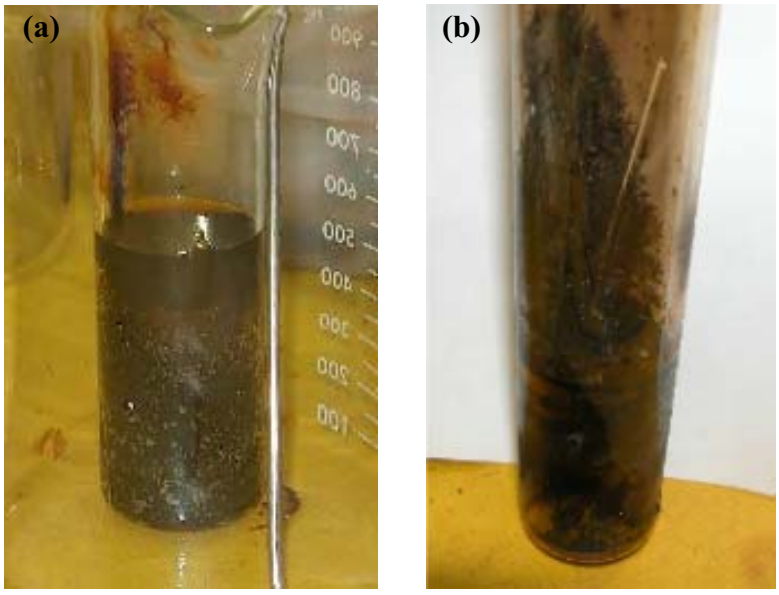

Fig. 14. HI_x phase separation upon cooling. (a) Feed and (b) boiler condition.

4.3. IMMERSION COUPON CORROSION TEST RESULTS

A total of 23 different materials have been tested. Ta, Nb and their alloys, along with SiC based materials have the best corrosion performance in HI_x. It was determined that the boiler condition is more corrosive than the feed condition probably due to the higher reaction temperature. Detailed discussion of the test results for each individual material is present in the following sections.

4.3.1. Ta

The Ta coupon appears to be very stable in the feed condition as the color variation is minimal and there is hardly any weight or thickness change at all (Fig. 15 and Table VIII). The color change is due to formation of a passivation layer which is the result of reaction between HI_x and the Ta coupon surface. This passivation proceeds at a higher rate under the boiler condition as noticeable color change can be observed in the specimen after 20 hours passivation. The coupon exhibits minor initial weight loss after 4 hours but remained essentially constant thereafter. The passivation is uniform through out the coupon except in the area around the hole which has a different shade. It is probably due to mechanical deformation in the material during machining. Close examination of the coupons revealed localized discoloration that may be a result of corrosion (Fig. 16). However, SEM analysis did not reveal any feature such as small pits corresponding to a corrosion event (Fig. 17). Hence, Ta is a viable material of construction candidate and may be used as a cladding material.

4.3.2. Ta-2.5W

Tungsten (W) is added to Ta to improve its high temperature creep property. Ta-2.5W and Ta-10-W are two common compositions. Ta-2.5W coupons with e-beam welds were tested at the boiler condition for 330 hours. A slight change in coupon color indicates the formation and growth of passivation. This passivation is more pronounced at the weld (Fig. 4.7). The thickness and weight of the specimen is basically unchanged (Table IX). Based on these findings, Ta-2.5W is a good material of construction candidate and more long term testing is planned.

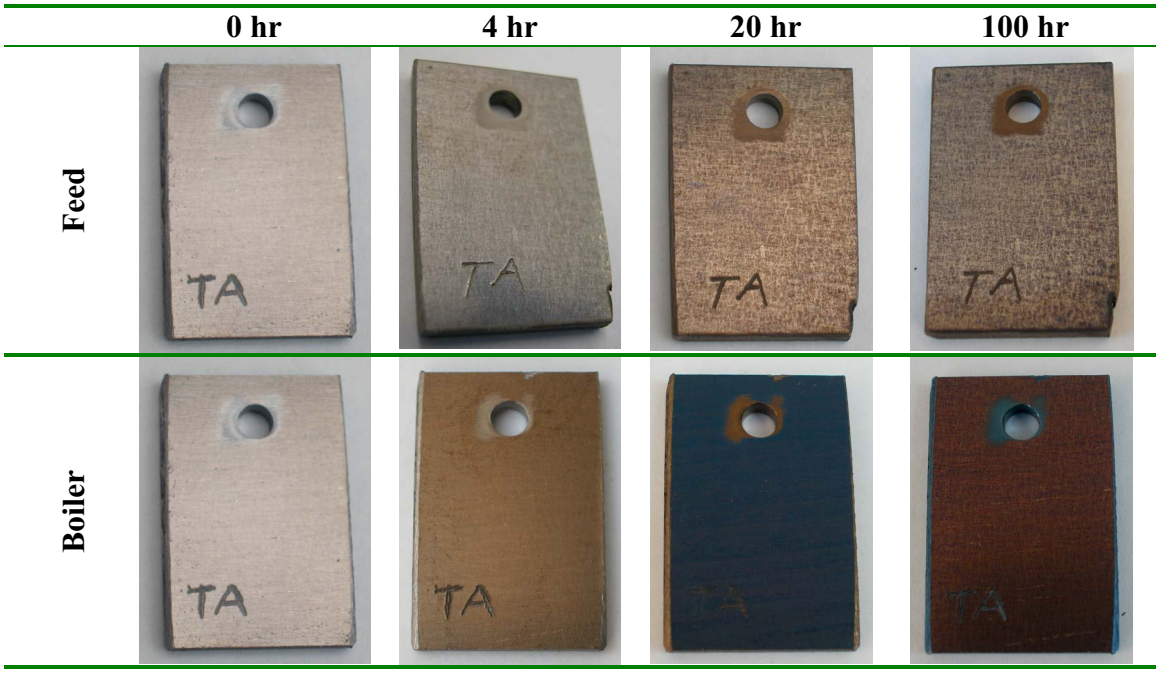

*The 0 hr feed coupon image is for reference only.

Fig. 15. Ta coupons tested at both the boiler and feed condition for 100 hrs.

Table VIII
Weight and Thickness Change of Ta Coupons Tested at Both the Feed and Boiler Condition

Ta (1) - Feed					
Duration (hr)	**PT 1**	**PT 2**	**PT 3**	**Avg. (in)**	**Weight (g)**
0	0.1331	0.1322	0.1329	0.1327	51.137
4	0.1331	0.1322	0.1329	0.1328	51.137
20	0.1331	0.1323	0.1330	0.1328	51.137
100	0.1332	0.1323	0.1329	0.1328	51.138

Ta (2) - Boiler					
Duration (hr)	**PT 1**	**PT 2**	**PT 3**	**Avg. (in)**	**Weight (g)**
0	0.1320	0.1326	0.1322	0.1323	51.010
4	0.1320	0.1326	0.1322	0.1323	51.005
20	0.1320	0.1325	0.1322	0.1323	51.004
100	0.1320	0.1325	0.1322	0.1323	51.004

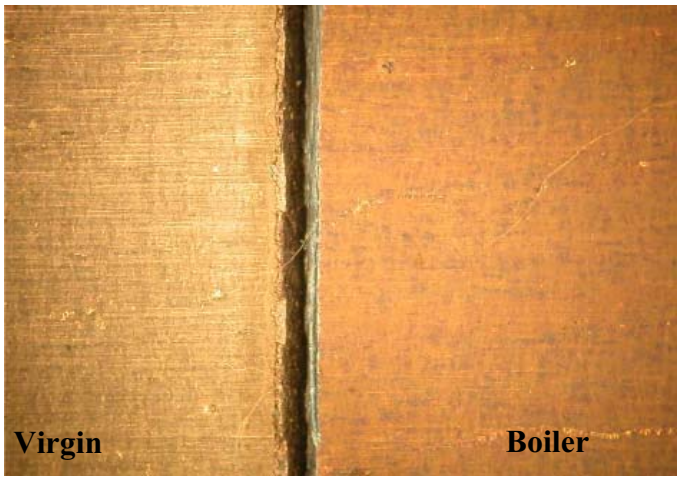

Fig. 16. Comparison between a Ta virgin and the boiler coupon.

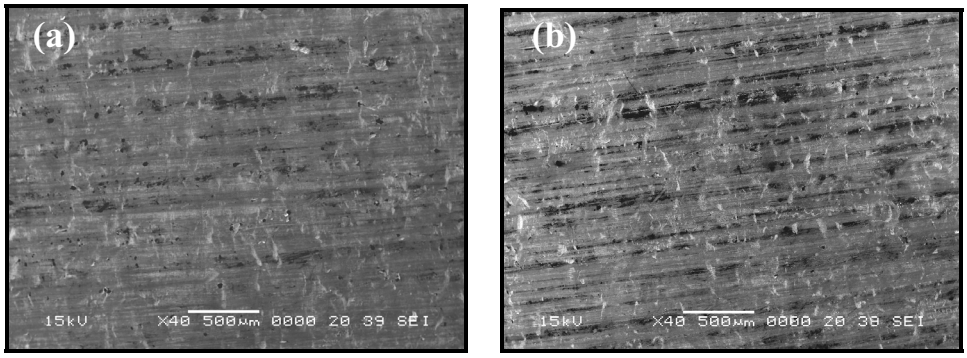

Fig. 17. SEM micrograph of the Ta coupons after 100 hr test. (a) boiler and (b) feed.

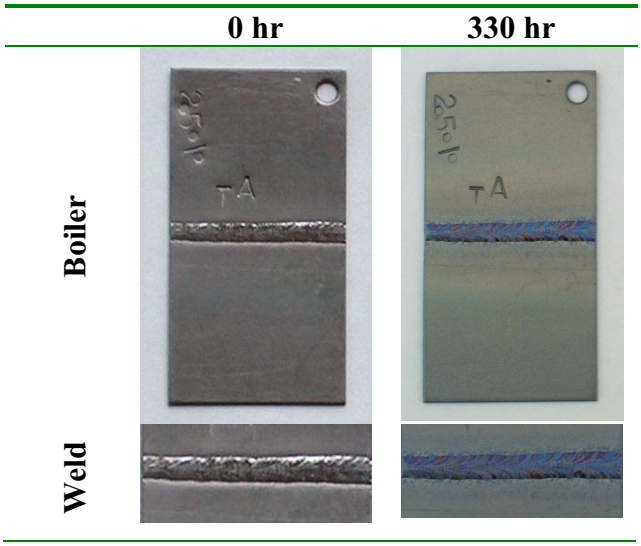

Fig. 18. Ta-2.5W coupon tested at the boiler condition for 330 hrs.

Table IX
Weight and Thickness Change of Ta-2.5W Coupons Tested at the Boiler Condition

	Ta-2.5W (1)				
Duration (hr)	**PT 1**	**PT 2**	**PT 3**	**Avg. (in)**	**Weight (g)**
0	0.0206	0.0211	0.0207	0.0208	11.829
330	0.0206	0.0212	0.0207	0.0208	11.830

4.3.3. Ta-10W

Ta-10W is another Ta alloy used to handle aggressive chemicals. Figure 19 shows the progression of Ta-10W samples from the immersion tests. At the feed condition, the sample shows no sign of corrosion and passivation is relatively thin. The passivation is more prominent at the boiler condition but the weight change is minimal (Table X). It shows Ta-10W has good corrosion resistance in HI_x and is a good candidate for development.

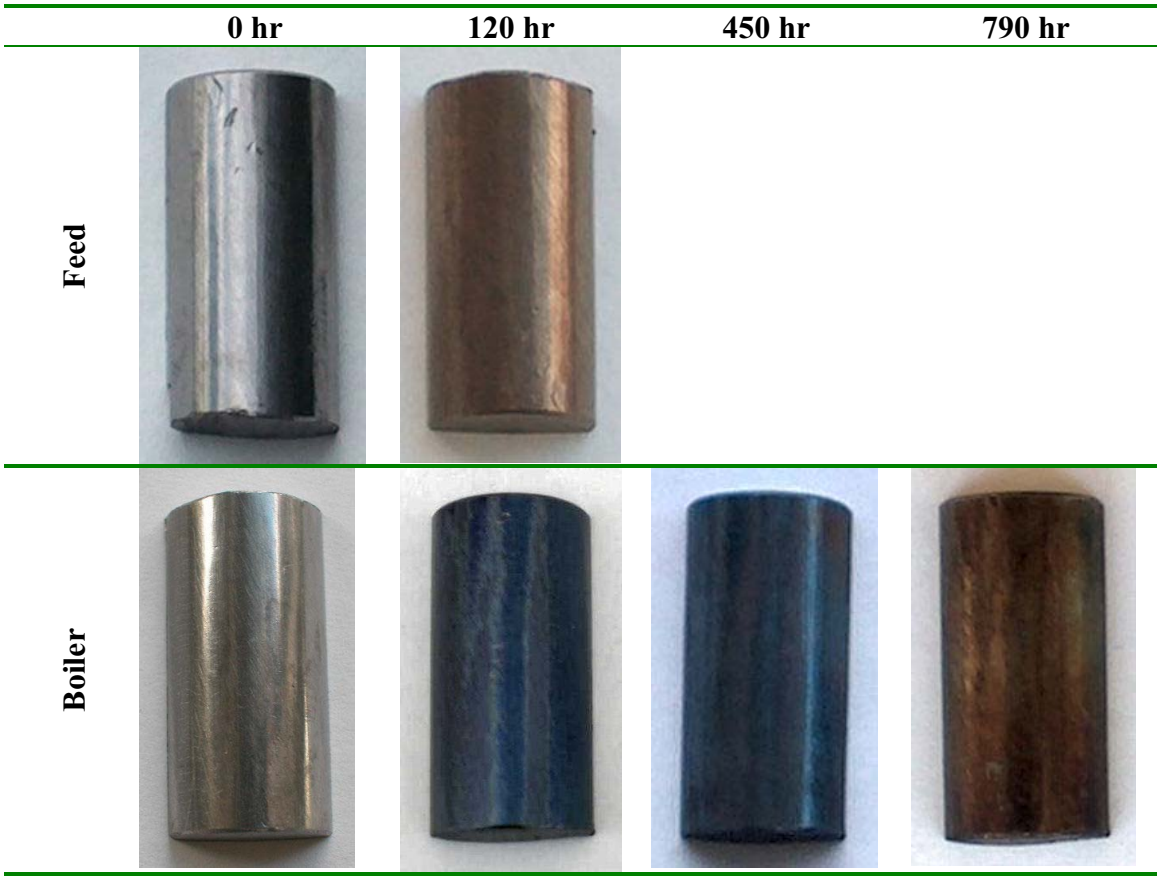

Fig. 19. Ta-10W coupons tested at the boiler and feed condition for 100 hrs.

Table X
Weight and Thickness Change of Ta-10W Specimens Tested at Both the Feed and Boiler Conditions

	Ta-10W (2) - Feed				
Duration (hr)	**PT 1**	**PT 2**	**PT 3**	**Avg. (in)**	**Weight (g)**
0	1.043	0.500	0.2684	0.6039	30.599
120	1.044	0.499	0.2664	0.6034	30.598

	Ta-10W (1) - Boiler				
Duration (hr)	**PT 1**	**PT 2**	**PT 3**	**Avg. (in)**	**Weight (g)**
0	1.042	0.491	0.20265	0.5784	21.354
120	1.042	0.491	0.199	0.5774	21.353
450	1.042	0.491	0.1992	0.5775	21.356
790	1.042	0.491	0.1995	0.5775	21.355

4.3.4. Ta-40Nb

A passivation layer built up with test time at both test conditions. The reaction rate is higher in the boiler coupon as indicated by the progression of the color changes (Fig. 20). The thickness and weight changes are not significant enough to draw any definite trend (Table XI).

One observation of note is the color of the boiler coupon after 100 hours of testing. It has a greenish metallic tint, which seems to indicate that the passivation layer has been removed. On the other hand, it is also reminiscence of color changes during Ti oxide film growth, which evolves from metallic to yellow to red to blue then to green as the thickness increases. It is imperative to compare the two coupons treated at both conditions to determine if the passivation layer is intact in the boiler specimen. This can provide insight into the effectiveness of Ta-40Nb as containment material.

Figure 21 shows the SEM microgrpahs. No sign of corrosion is present in either coupons. This indicates that Ta-40Nb is be a good development candidate for the HI reactive distillation decomposition process.

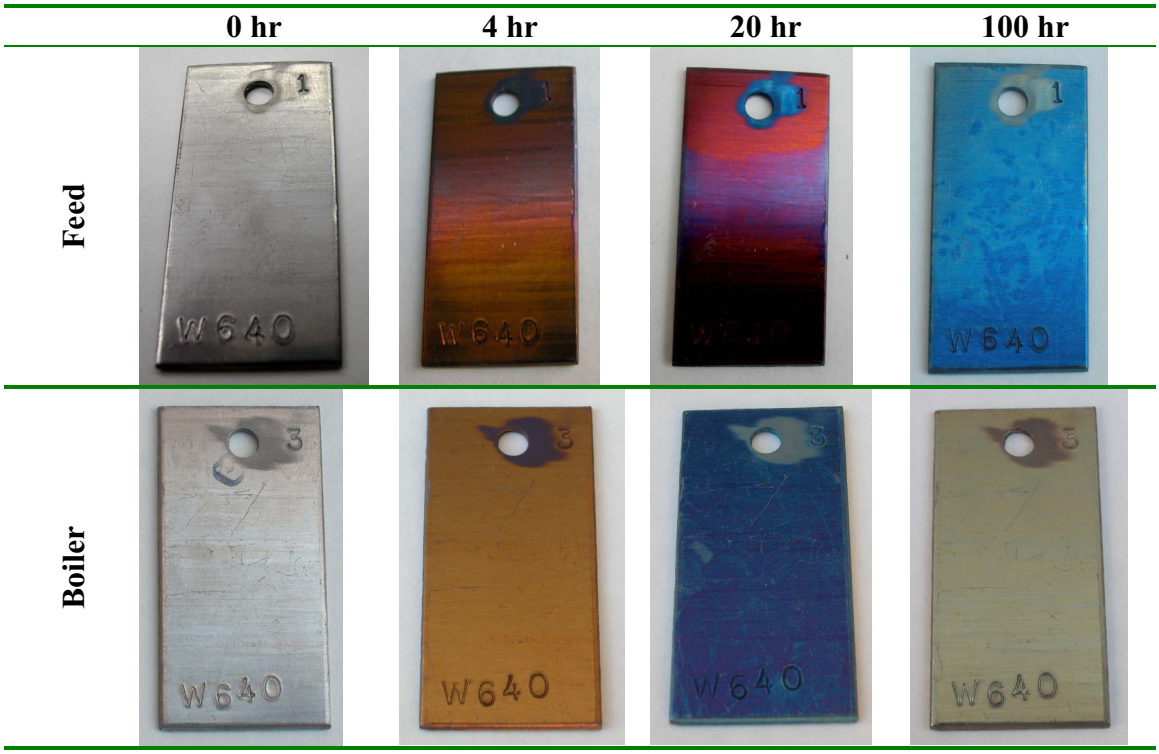

Fig. 20. Ta-40Nb coupons tested at both the boiler and feed condition for 100 hrs.

Table XI
Weight and Thickness Change of Ta-40Nb Coupons Tested at Both the Feed and Boiler Condition

Ta-40Nb (1) - Feed					
Duration (hr)	**PT 1**	**PT 2**	**PT 3**	**Avg. (in)**	**Weight (g)**
0	0.0616	0.0611	0.0611	0.0613	23.026
4	0.0617	0.0610	0.0613	0.0613	23.025
20	0.0617	0.0612	0.0613	0.0614	23.024
100	0.0618	0.0612	0.0613	0.0614	23.025

Ta-40Nb (3) - Boiler					
Duration (hr)	**PT 1**	**PT 2**	**PT 3**	**Avg. (in)**	**Weight (g)**
0	0.0602	0.0613	0.0613	0.0609	23.488
4	0.0602	0.0613	0.0612	0.0609	23.490
20	0.0602	0.0612	0.0612	0.0609	23.490
100	0.0602	0.0612	0.0614	0.0609	23.491

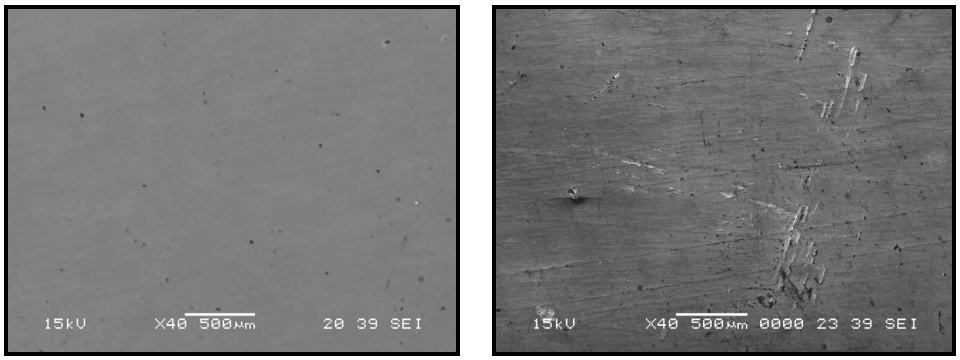

Fig. 21. SEM micrograph of the Ta-40Nb coupons after 100 hr test. (a) boiler and (b) feed

4.3.5. Nb

Nb is a commonly employed in corrosive environment for its resistant against a variety of chemicals, especially in aqueous environment. Its corrosion resistance to acid at high temperature can be improved immensely by alloying. The coherent oxides are able to withstand hot and concentrated acid. Figure 22 shows the Nb coupons tested at both the feed and boiler conditions. Once again, the passivation developed much faster in the boiler coupon as shown by its much darker color. There is also a minor increase in the boiler coupon weight probably due to oxygen pick up in the passivation (Table XII). Nb can be a material candidate but Nb alloy is most likely a better option.

4.3.6. Nb-1Zr

The Nb-1Zr coupons show excellent corrosion performance up to 120 hours at both conditions (Fig. 23 and Table XIII). However, extensive corrosion is observed after 450 hours in the boiler environment. The circumstance surrounding the experiment was unusual since the glass wool used to minimize HI_x vaporization was found inside the HI_x liquid. It was suspected that contamination from the glass wool had caused the corrosion. The corrosion product has been saved for analysis and detail characterization of the coupon will be conducted at UNLV.

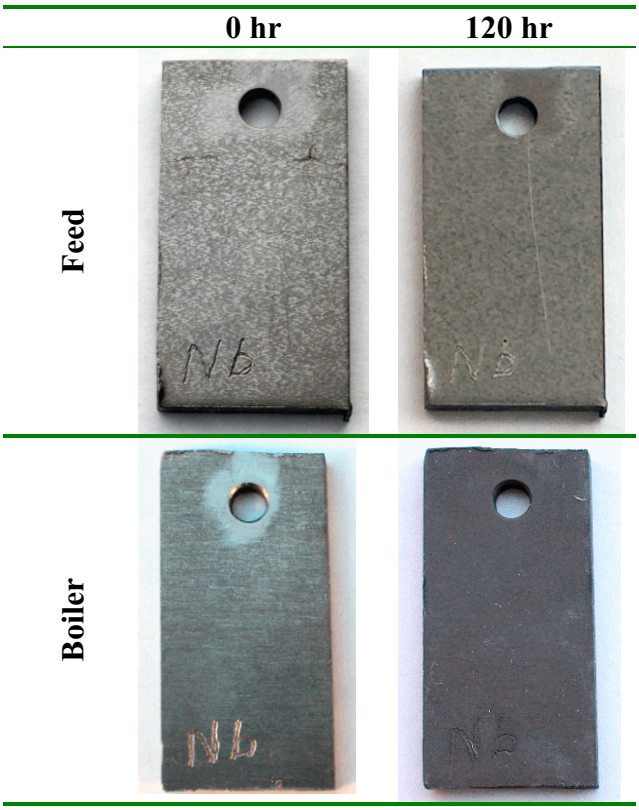

Fig. 22. Nb coupons tested at both the boiler and feed condition for 120 hrs.

Table XII
Weight and Thickness Change of Nb Coupons Tested at the Feed and Boiler Conditions

			Nb (2) - Feed		
Duration (hr)	**PT 1**	**PT 2**	**PT 3**	**Avg. (in)**	**Weight (g)**
0	0.127	0.128	0.1271	0.1273	26.508
120	0.127	0.127	0.12725	0.1273	26.508

			Nb (1) - Boiler		
Duration (hr)	**PT 1**	**PT 2**	**PT 3**	**Avg. (in)**	**Weight (g)**
0	0.128	0.128	0.12765	0.1276	27.195
120	0.128	0.128	0.1278	0.1278	27.198

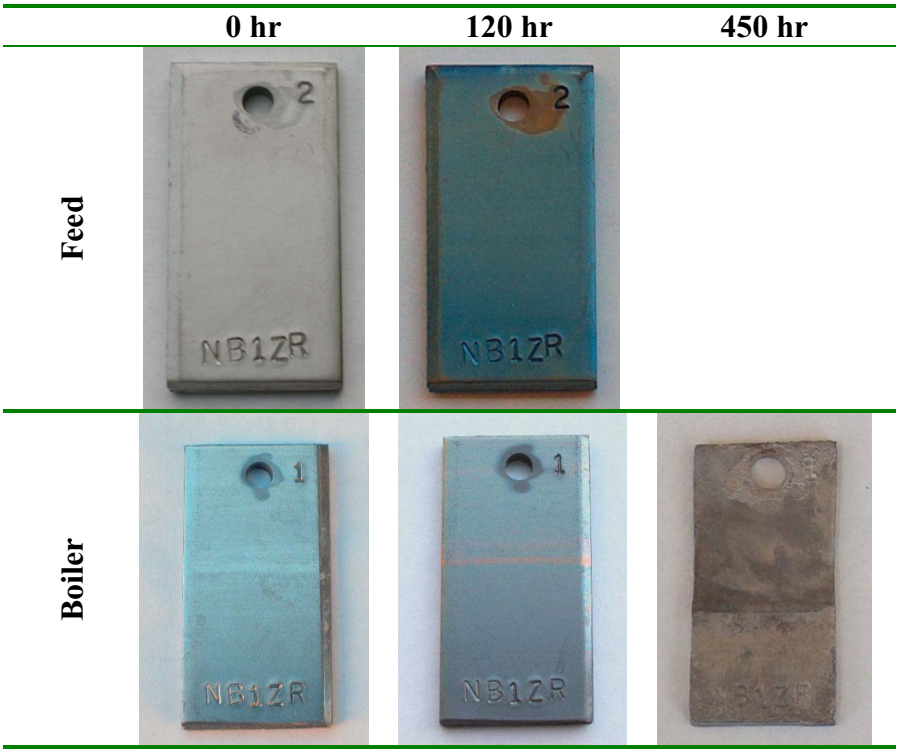

Fig. 23. Nb-7.5 Ta coupons tested at both the boiler and feed condition for 100 hrs.

Table XIII
Weight and Thickness Change of Nb-1Zr Coupons
Tested at the Both Feed and Boiler Conditions

Nb-1Zr (2) - Feed					
Duration (hr)	**PT 1**	**PT 2**	**PT 3**	**Avg. (in)**	**Weight (g)**
0	0.135	0.135	0.1354	0.1353	37.588
120	0.135	0.135	0.1355	0.1353	37.586

Nb-1Zr (1) - Boiler					
Duration (hr)	**PT 1**	**PT 2**	**PT 3**	**Avg. (in)**	**Weight (g)**
0	0.135	0.135	0.1352	0.1353	37.302
120	0.135	0.136	0.13515	0.1353	37.303
450	0.084	0.067	0.09975	0.0836	19.700

To test this postulation, an experiment was conducted by wrapping a new coupon with glass wool and submerged in HI_x for testing (Fig. 24). Figure 25 shows the resultant coupon in which no corrosion can be observed. Correspondingly, the weight change is minimal (Table XIV). The reason behind the unexpected corrosion is still under

investigation. Further testing is required if one wants to use Nb-1Zr as heat exchanger construction material.

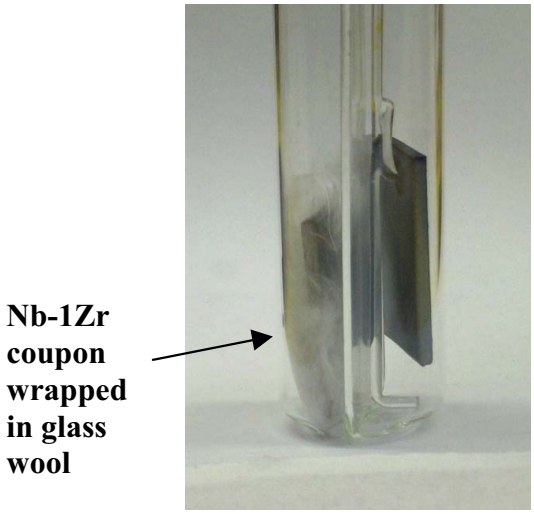

Fig. 24. Immersion coupon testing with a Nb-1Zr coupon wrapped in glass wool. Another coupon was also tested simultaneously as a reference.

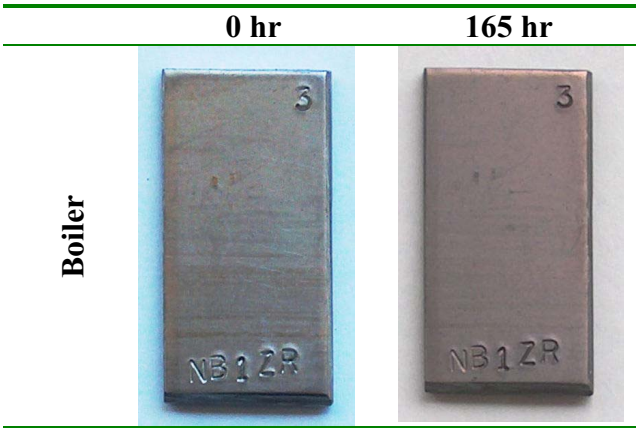

Fig. 25. Nb-1Zr coupon wrapped in glass wool and tested at the boiler condition for 165 hrs.

Table XIV
Weight and Thickness Change of Nb-1Zr Coupon Wrapped in Glass Wool and Tested at the Boiler Condition

	Nb-1Zr (3) - Boiler				
Duration (hr)	**PT 1**	**PT 2**	**PT 3**	**Avg. (in)**	**Weight (g)**
0	0.135	0.135	0.1367	0.1358	37.956
165	0.136	0.136	0.1355	0.1356	37.958

4.3.7. Nb-7.5Ta

The Nb-7.5Ta immersion coupons are shown in Fig. 26 and the corresponding change in thickness and weight are listed in Table XV. The color of the coupons changed uniformly from metallic to blue and then to an orange rusty color as testing progresses which indicates a reaction between the coupons and HI_x. The initial color changes are due to optical interference but after this surface passivation is thicker than the wavelength of light; the true color of the film becomes apparent. This even passivation is essential to protect the coupons from HI_x as it acts as a protective barrier and it is critical that it adheres well to the metal. The nature of this passivation is not known and will require an analytical analysis. It could be either be an oxide layer, an iodide layer or a complex of the two. It is important to understand the formation and growth mechanism of this layer as it provides an insight to the corrosion mechanism and thus means to counter it.

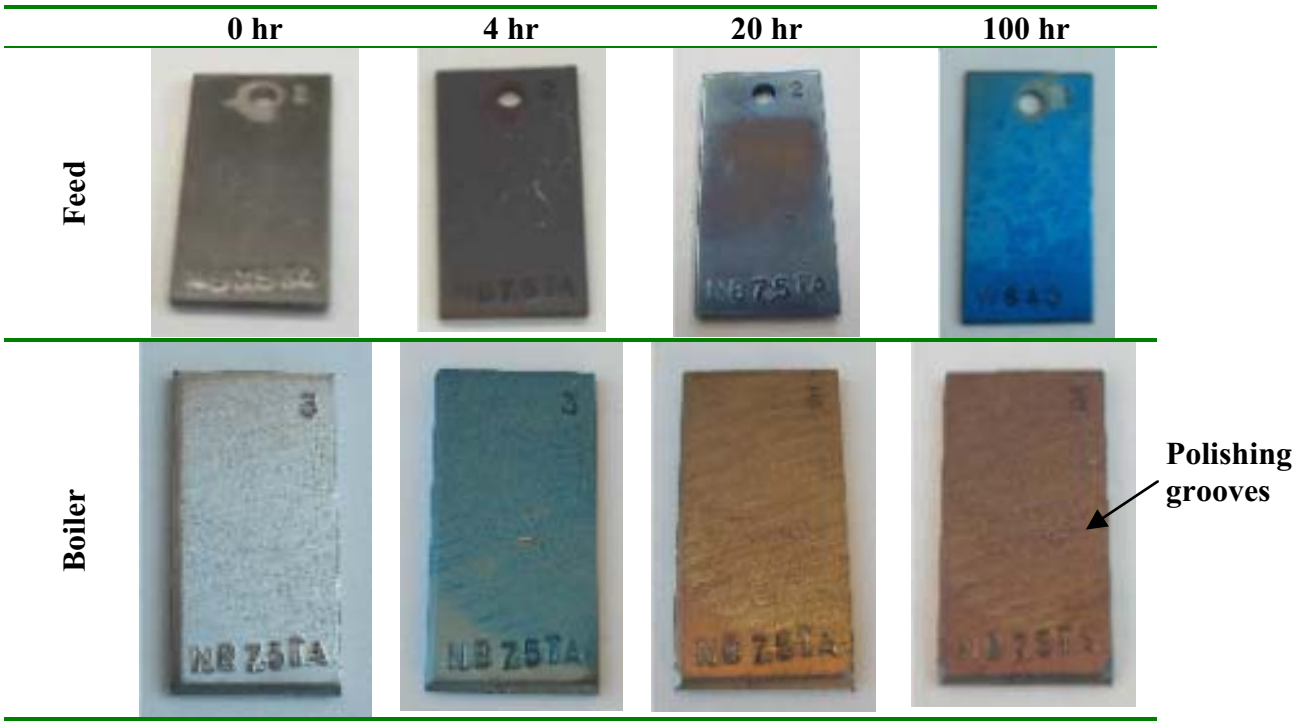

Fig. 26. Nb-7.5 Ta coupons tested at the boiler and feed condition for 100 hrs.

The thickness and weight change is minimal in the two coupons as they fall within the uncertainty of the measurement. Weight change is small due to the limited test duration. For the boiler-composition coupon, the weight seems to exhibit a small decline. Unfortunately, the sample was damaged during retrieval after 20 hours that led to a loss in material. It is difficult to calculate a meaningful corrosion rate and draw any concrete conclusion without a longer immersion test.

Table XV
Weight and Thickness Change of Nb-7.5Ta Coupons Tested at Both the Feed and Boiler Conditions

Nb-7.5Ta (2) - Feed					
Duration (hr)	**PT 1**	**PT 2**	**PT 3**	**Avg. (in)**	**Weight (g)**
0	0.1182	0.1180	0.1177	0.1180	34.23
4	0.1182	0.1180	0.1177	0.1180	34.23
20	0.1180	0.1177	0.1176	0.1177	34.229
100	0.1181	0.1180	0.1176	0.1179	34.233

Nb-7.5Ta (3) -Boiler					
Duration (hr)	**PT 1**	**PT 2**	**PT 3**	**Avg. (in)**	**Weight (g)**
0	0.1180	0.1178	0.1181	0.1180	34.718
4	0.1180	0.1178	0.1181	0.1180	34.716
20	0.1181	0.1179	0.1182	0.1181	34.692
100	0.1181	0.1179	0.1182	0.1181	34.688

Upon closer examination of the surface of the boiler-composition coupon, pits can be observed on parts of the surface covered with polishing grooves. Figure 27 shows magnified images of surface of the different Nb-7.5Ta specimens. The virgin and the feed specimens show essentially the same surface finish. Figure 27(c) shows the surface morphology from the smooth portion of the boiler coupon. Small areas of discoloration, possibly due to corrosion, can be observed. Figures 27(d) and 28 show severe pitting on the part of the coupon which was covered with polishing marks (also Fig. 26). This helps to illustrate the effect of deformation on the corrosion properties of materials. The plastic strain caused by the polishing and the corrosion environment together accelerated the process, which resulted in severe pitting. It also demonstrates the importance in testing not only plain coupons but also specimens that have been physically processed. Nb-7.5Ta can be a development candidate but it will require more testing to verify the origin of the pits.

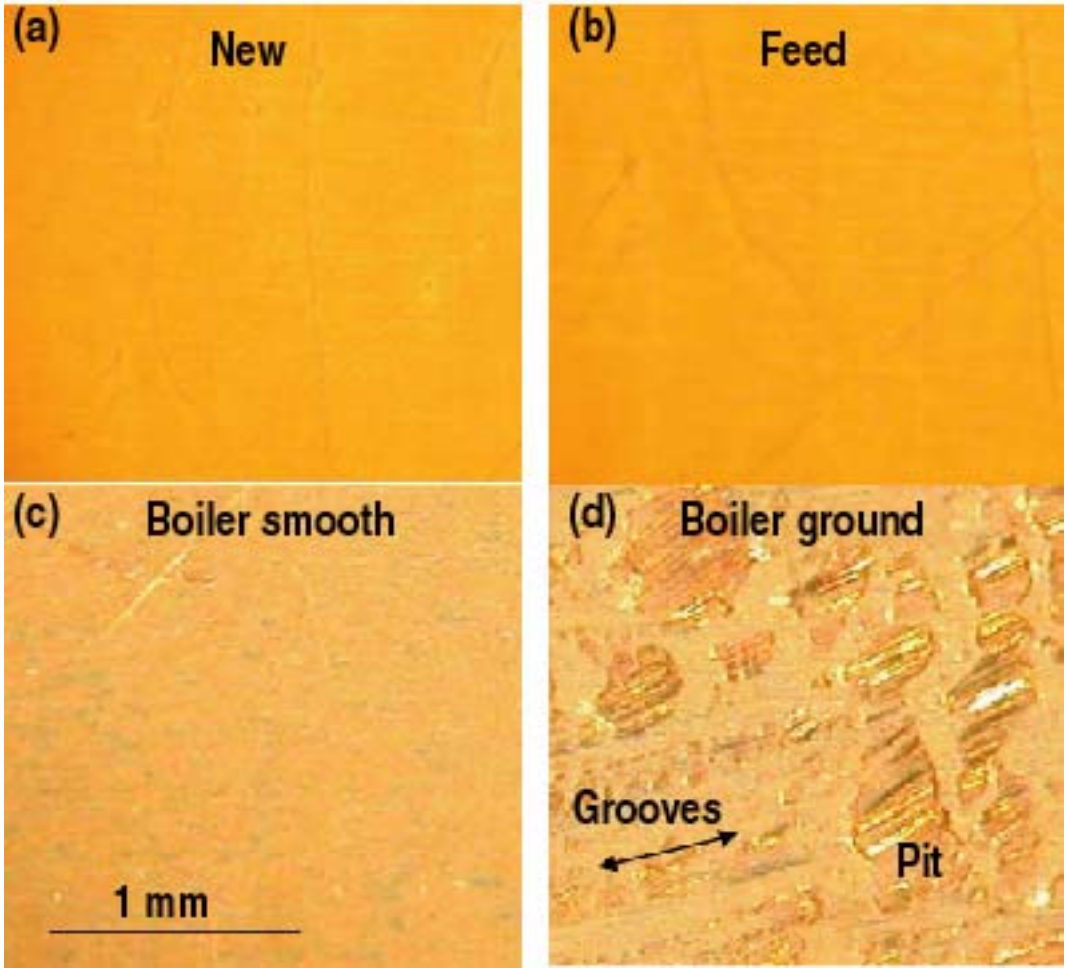

Fig. 27. Optical micrographs showing the effect of polishing grooves on pit formation on Nb-7.5Ta coupon surface. (a) new, (b) feed coupon after 100 hrs, (c) boiler coupon smooth area and (d) boiler coupon polished area after 100 hrs.

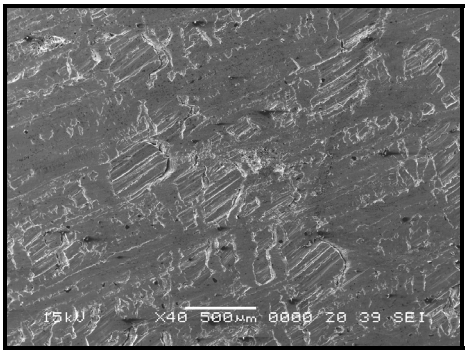

Fig. 28. SEM micrograph showing corrosion pit in Nb-7.5Ta boiler coupon.

4.3.8. Nb-10Hf

Nb-10Hf is a commercially available high temperature alloy and is appropriate for corrosive environment. Both screening and the subsequent long term testing of Nb-10Hf show that the alloy is stable in HI_x as the coupons do not exhibit any sign of corrosion (Fig. 29). The results (Table XVI) indicate the passivation is still undergoing changes even after 790 hrs. Long term testing obtained so far reveals that Ta-2.5W, Ta-10W and Nb-10Hf are leading materials of construction candidates for HI decomposition whereas the use of Nb-1Zr will need to be examined carefully.

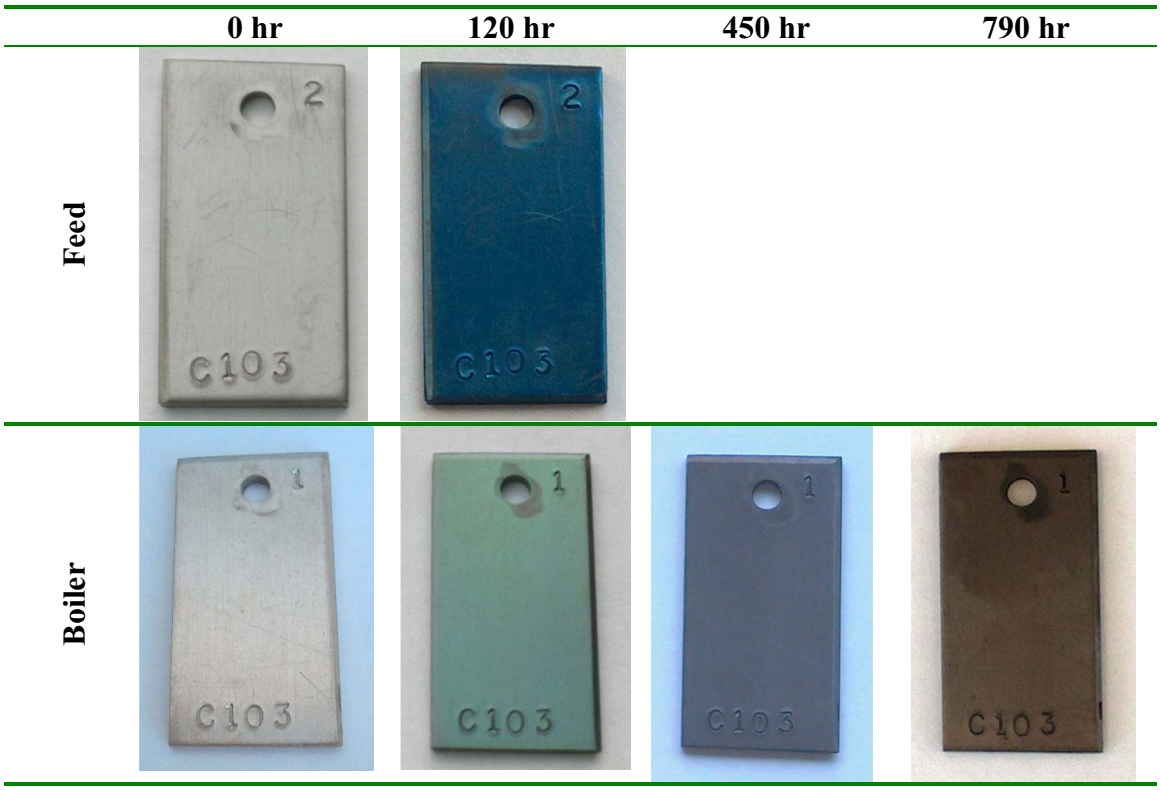

Fig. 29. Nb-10Hf coupons tested at both the boiler and feed condition.

Table XVI
Weight andThickness Change of Nb-10Hf Coupons
Tested at Both the Feed and Boiler Conditions

Nb-10Hf (2)- Feed					
Duration (hr)	**PT 1**	**PT 2**	**PT 3**	**Avg. (in)**	**Weight (g)**
0	0.099	0.105	0.105	0.1028	28.426
120	0.099	0.104	0.10505	0.1028	28.426

Nb-10Hf (1) - Boiler					
Duration (hr)	**PT 1**	**PT 2**	**PT 3**	**Avg. (in)**	**Weight (g)**
0	0.104	0.104	0.1021	0.1034	28.1809
120	0.104	0.104	0.102	0.1034	28.181
450	0.105	0.104	0.10195	0.1034	28.183
790	0.105	0.104	0.1021	0.1034	28.184

4.3.9. Mo

Molybdenum is known to have good resistance against a variety of acid under 100°C. However, the coupon test in the boiler condition is corroded and exhibits weight loss (Fig. 30 and Table XVII). Hence, Mo is not applicable to this environment.

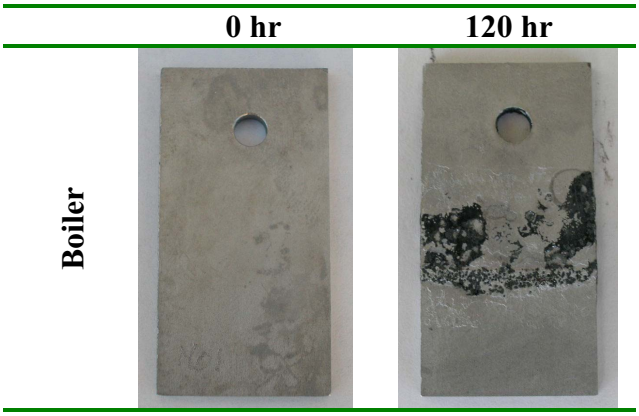

Fig. 30. Mo coupon tested at the boiler condition for 120 hr.

Table XVII
Weight and Thickness Change of Mo Coupon Tested at the Boiler Condition

Mo (1)					
Duration (hr)	**PT 1**	**PT 2**	**PT 3**	**Avg. (in)**	**Weight (g)**
0	0.101	0.100	0.10075	0.1004	29.285
120	0.095	0.098	0.0878	0.0938	25.683

4.3.10. Mo-47Re

Mo-Re alloys have high temperature resistance and are used for space power application. After testing in the boiler condition, the specimen is stable (Fig. 31). There is a minor weight loss but can be significant with respect to the weight of the specimen (Table XVIII). This shows that Mo-Re alloys may not suitable for HI decomposition application.

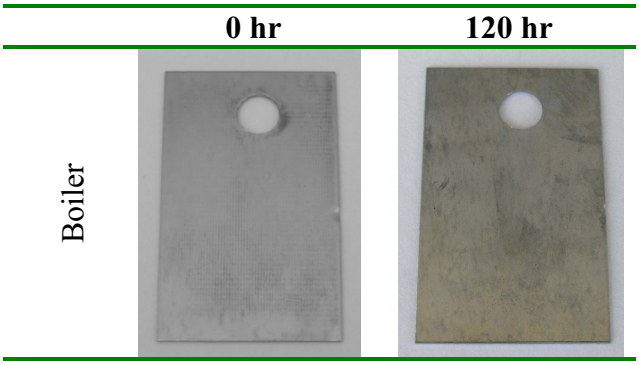

Fig. 31. Mo-47Re coupon tested at the boiler condition for 120 hr.

Table XVIII
Weight and Thickness Change of Mo-47Re Coupon Tested at the Boiler Condition

	Mo-Re (1)				
Duration (hr)	**PT 1**	**PT 2**	**PT 3**	**Avg. (in)**	**Weight (g)**
0	0.017	0.016	0.01645	0.0164	6.083
120	0.017	0.016	0.0166	0.0165	6.076

4.3.11. Zr 702

Zr702 and Zr705 are widely used in the chemical and nuclear industry for their corrosion resistance. For the present test, the feed coupon did not exhibit any large scale corrosion (Fig. 32). The thickness of the passivation layer on the coupon is not uniform (based on color distribution) which is not desirable (Table XIX). Closer examination of the coupon reveals the presence of small pits in parts of the coupons. Figure 33(a) shows a comparison between a virgin coupon and the feed coupon where rows of small pits can be found in the later sample. A magnified image of the pits is shown in Fig. 33(b). Hence, more corrosion will probably occur in this coupon at longer test time.

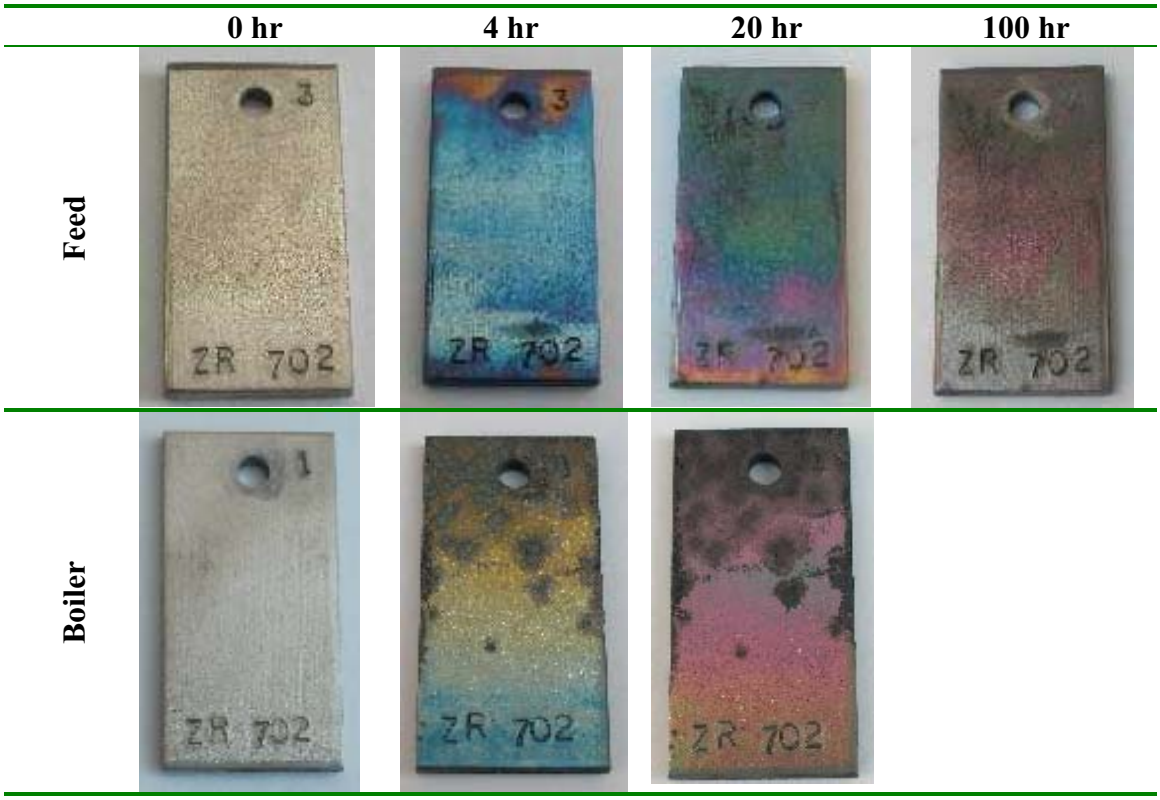

Fig. 32. Zr702 coupons tested at the feed and the boiler condition for 100 and 20 hrs respectively.

Table XIX
Weight and Thickness Change of Nb-7.5Ta Coupons Tested at the Feed and Boiler Conditions

			Zr702 (3)		
Duration (hr)	**PT 1**	**PT 2**	**PT 3**	**Avg. (in)**	**Weight (g)**
0	0.1480	0.1481	0.1480	0.1480	31.262
4	0.1480	0.1481	0.1479	0.1480	31.262
20	0.1480	0.1481	0.1480	0.1480	31.263
100	0.1480	0.1480	0.1480	0.1480	31.265

			Zr702 (1)		
Duration (hr)	**PT 1**	**PT 2**	**PT 3**	**Avg. (in)**	**Weight (g)**
0	0.1475	0.1480	0.1479	0.1478	31.312
4	0.1474	0.1478	0.1480	0.1477	30.76
20	0.1473	0.1478	0.1486	0.1479	30.757

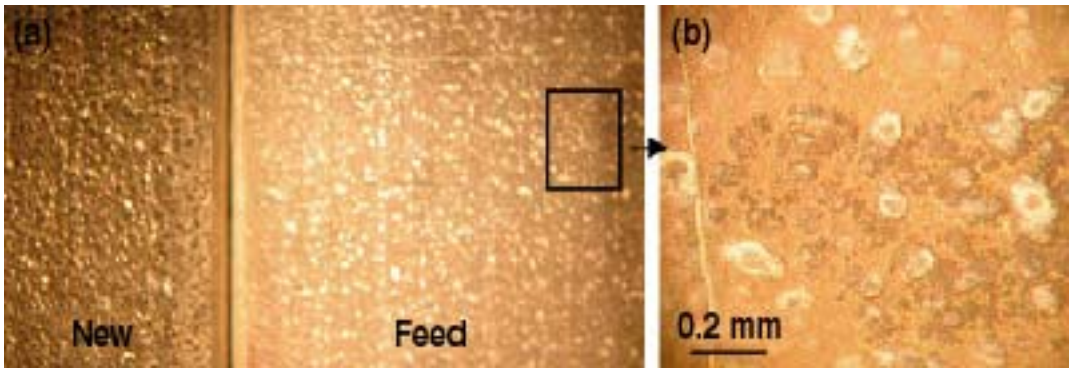

Fig. 33. Onset of small scale pitting corrosion in the Zr702 coupon tested at the fed condition.

Severe attack can be observed in the boiler-composition coupon (Fig. 32 and 34). Pitting and dissolution have been initiated in the specimen only after 4 hours. Between hour 4 and hour 20, the corrosion proceeded at a slower rate as the pit size and the corroded area only increased moderately. The loss of material is reflected by the weight reduction. The original accelerated corrosion could be the true characteristics of Zr702 or it may have due to contaminants of other species. For example, pitting has been observed in Zr in the halide environments where oxidizing Fe or Cu ions are present from 4 to 20 hours. However, such corrosion is not acceptable as cross contamination of corrosion products as expected to occur between the different sections of the SI cycle. Hence, Zr702 is not suitable for HI decomposition. Testing was terminated after 20 hours as the specimen was severely corroded.

4.3.12. Zr705

Zr705 behavior in HI_x is similar to Zr702. Extensive corrosion and dissolution of the coupon took place during the test (Fig. 35 and Table XX). It is interesting to note that the dissolution takes place only at the bottom of the coupon. This may indicate a chemical gradient within the HI_x test medium. From the immersion test results, it is clear that both Zr702 and Zr705 are not desirable candidates for HI decomposition components.

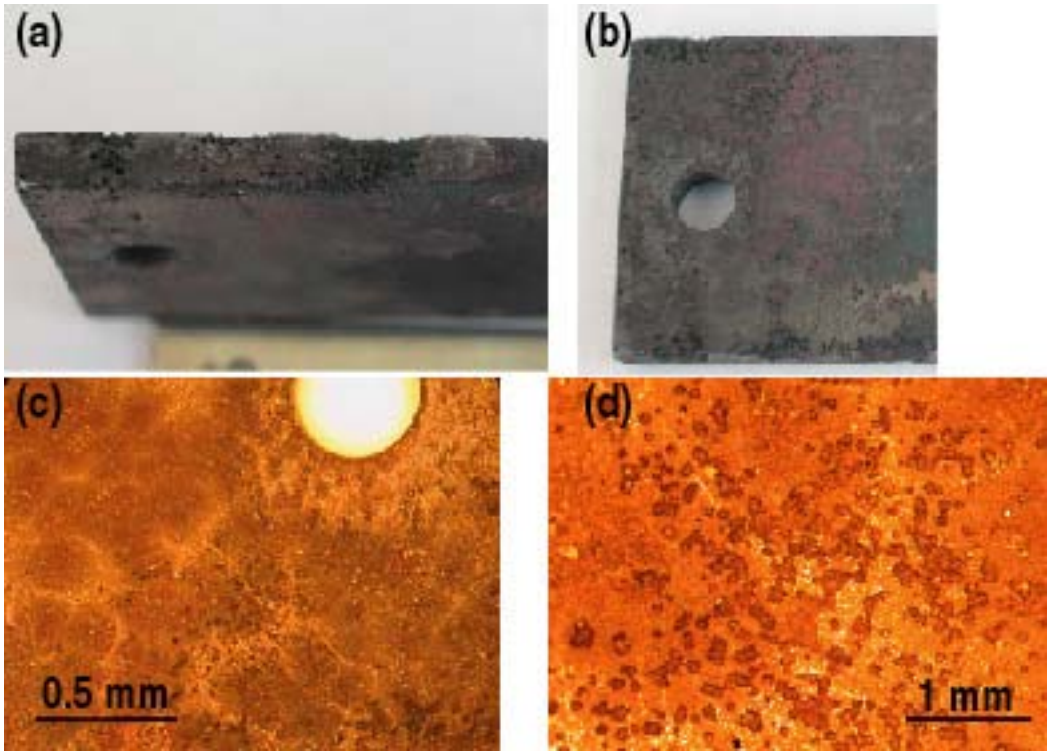

Fig. 34. (a–d) Micrographs showing extensive pitting corrosion found in the Zr-702 coupon test at the boiler condition.

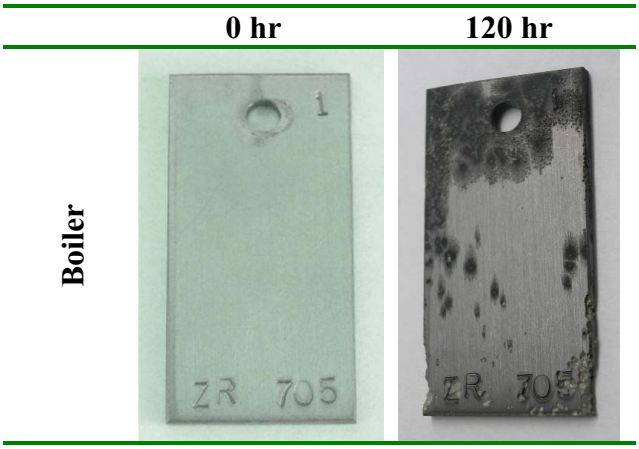

Fig. 35. Zr705 coupon tested at the boiler condition for a 120 hr.

Table XX
Weight and Thickness Change of Zr705 Coupon Tested at the Boiler Condition

	Zr705 (1)				
Duration (hr)	**PT 1**	**PT 2**	**PT 3**	**Avg. (in)**	**Weight (g)**
0	0.1179	0.1174	0.1168	0.1173	25.11
120	0.1174	0.1174	0.1168	0.1172	24.58

4.3.13. C-276

C-276, a Ni-based superalloy, has been shown to have excellent corrosion properties in numerous applications. However, its corrosion resistance in HI_x is extremely poor. Figure 36 shows the coupon before and after the test. The coupon has a weight loss of 31% reflecting severe dissolution of the material (Table XXI). Hence, the protective transition metal oxide is not effective in the HI_x environment and Ni-based superalloys are not suitable for this use.

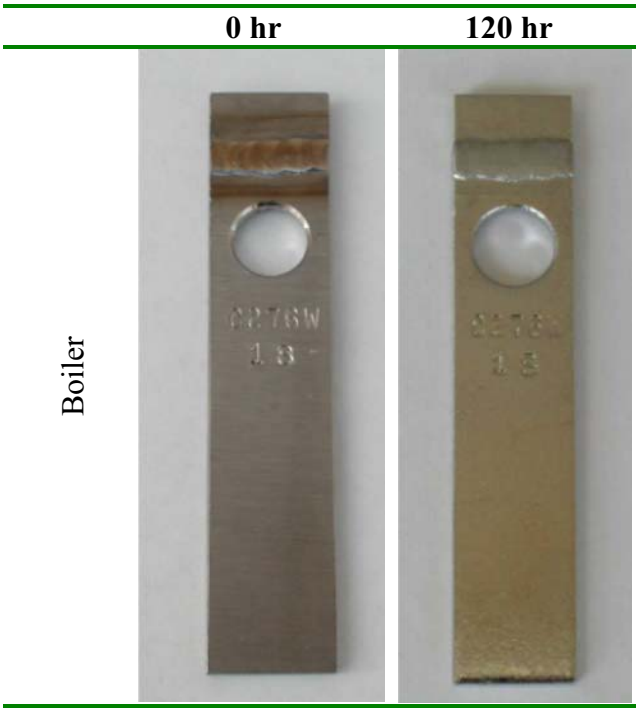

Fig. 36. C-276 coupon tested at the boiler condition for 120 hr.

Table XXI
Weight and Thickness Change of C-276 Coupon Tested at the Boiler Condition

	C276 (18)				
Duration (hr)	**PT 1**	**PT 2**	**PT 3**	**Avg. (in)**	**Weight (g)**
0	0.1215	0.1206	0.1206	0.1209	30.854
120	0.0844	0.0857	0.0813	0.0838	21.257

4.3.14. Haynes 188

Haynes 188, a Co-based alloy, is also a widely used as corrosion resistant material. However, just like C-276, extensive dissolution took place during the immersion test which disqualifies it for any HI decomposition application (Fig. 37 and Table XXII).

Fig. 37. Haynes 188 coupon tested at the boiler condition for 120 hr.

Table XXII
Weight and Thickness Change of C-276 Coupon tested at the Boiler Condition

	Haynes 188 (20)				
Duration (hr)	**PT 1**	**PT 2**	**PT 3**	**Avg. (in)**	**Weight (g)**
0	0.1258	0.1240	0.1245	0.1248	32.131
120	0.1145	0.1129	0.1104	0.1126	28.41

4.3.15. SiC (Sintered)

SiC has good corrosion resistance in almost any environment. Furthermore, it has high thermal conductivity which makes it an ideal material for HI heat exchanger applications. A commercially available sintered SiC heat exchanger tube specimen was test in HI. There was no discoloration after immersion (Fig. 38). There is no sign of corrosion but a measurable weight loss is recorded (Table XXIII). The weight reduction is mostly likely caused by small pieces chipping off the specimen as SiC is a very brittle material.

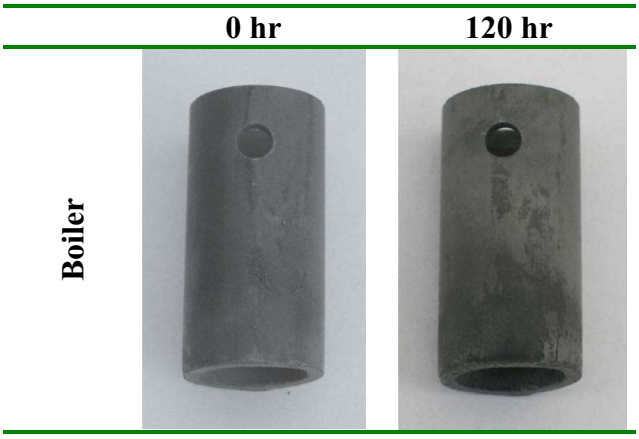

Fig. 38. Sintered SiC tubing tested at the boiler condition for a 120 hr.

Table XXIII
Weight and Thickness Change of Sintered SiC Sample Tested at the Boiler Condition

	SiC Sintered Commercial				
Duration (hr)	**PT 1**	**PT 2**	**PT 3**	**Avg. (in)**	**Weight (g)**
0	0.750	0.092	1.486	0.7759	13.318
120	0.749	0.092	1.485	0.7752	13.307

4.3.16. Ceramatec SiC (Sintered)

Another sintered SiC coupon from Cerematec was also tested in HI_x (Fig. 39 and Table XXIV). The coupon after test is very clean and the amount of chipping is in general less than the other specimen. The reason may be a result that the binding agent for the sintering process is different between the two samples.

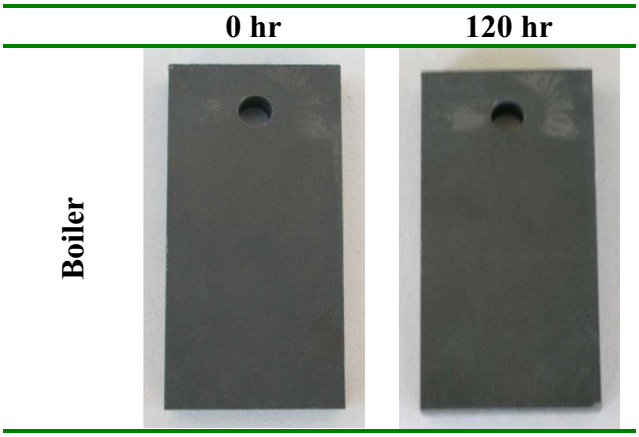

Fig. 39. Sintered SiC (Cermatec) tubing tested at the boiler condition for a 120 hr.

Table XXIV
Weight and Thickness Change of Sintered SiC Sample Tested at the Boiler Condition

	SiC Sintered (Cerametec)				
Duration (hr)	**PT 1**	**PT 2**	**PT 3**	**Avg. (in)**	**Weight (g)**
0	0.273	0.274	0.272	0.2731	28.954
120	0.274	0.274	0.2719	0.2732	28.950

4.3.17. SiC (CVD)

SiC can also be made by chemical vapor deposition (CVD). CVD SiC coupons were tested in HI_x at both the feed and boiler condition and the coupons came through the test without any sign of corrosion (Fig. 40). The small weight loss is probably related to small chips falling off, which is a problem with ceramic materials (Table XXV). In any event, it shows that it is possible to coat material with SiC and use them in HI decomposition.

All the monolithic SiC samples tested showed excellent resistance in HI_x but their application will be limited by the ability to process them and build components with it. Manufacturing techniques are being developed to address such issues. More long term

testing will be conducted as SiC will most likely be used in future generation of heat exchanger for the S-I process.

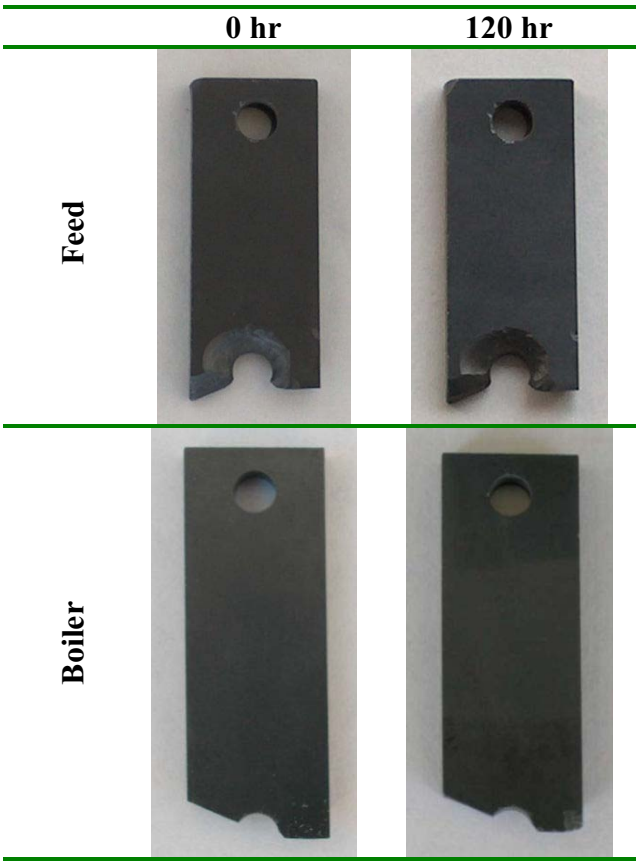

Fig. 40. CVD SiC coupons tested at both the feed and boiler condition for a 120 hr.

Table XXV
Weight and Thickness Change of CVD SiC Coupons Tested at the Feed and Boiler Conditions

CVD SiC (2) - Feed					
Duration (hr)	**PT 1**	**PT 2**	**PT 3**	**Avg. (in)**	**Weight (g)**
0	0.161	0.161	0.1615	0.1614	6.759
120	0.162	0.162	0.16165	0.1616	6.758

CVD SiC (1) - Boiler					
Duration (hr)	**PT 1**	**PT 2**	**PT 3**	**Avg. (in)**	**Weight (g)**
0	0.162	0.162	0.16155	0.1616	7.995
120	0.162	0.162	0.1616	0.1617	7.994

4.3.18. Bioker 29 Si-SiC

Si-SiC composite provides a possible economic means to construct ceramic heat exchangers. It is made simply by infiltrating pyrolysed wooden templates with liquid Si at high temperature. Si-SiC composite fabricated this way has high density and is corrosion resistant [10,11]. Three such specimens, Bioker 29, splint and fiber, have been tested in HI_x (Fig. 41 and Table XXVI). The main difference between them is the starting material and resin that were used. The Bioker 29 coupon showed no sign of corrosion after testing in HI_x. A corner piece that had been glued onto the specimen had fallen off. If it weren't for that, the weight change would have been minimal gauged by the surface morphology of the specimen.

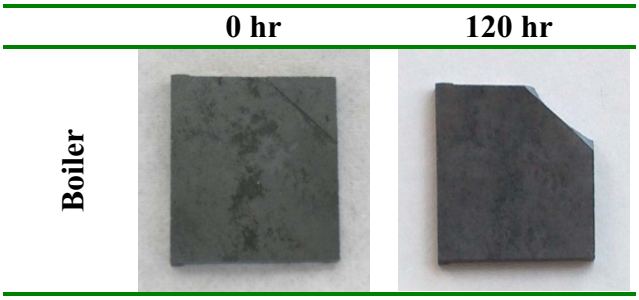

Fig. 41. Bioker 29 Si-SiC coupon tested at the boiler condition for 120 hr.

Table XXVI
Weight and Thickness Change of Sintered Bioker 29 Si-SiC Coupons Tested at the Boiler Condition

	Bioker 29				
Duration (hr)	**PT 1**	**PT 2**	**PT 3**	**Avg. (in)**	**Weight (g)**
0	0.119	0.119	0.1188	0.1187	7.581
120	0.119	0.119	0.1188	0.1186	7.013*

*Corner piece not included.

4.3.19. Splint Si-SiC

Splint Si-SiC was tested at both the boiler and feed conditions (Fig. 41 and Table XXVII). The specimens are very stable in HI_x with no evidence of any corrosion. This is probably due to the higher SiC content within the matrix.

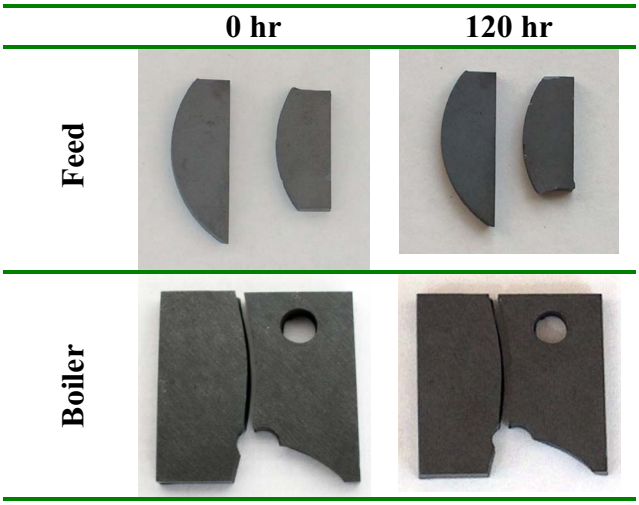

Fig. 42. Splint Si-SiC sample tested at both the feed and boiler condition for 120 hr.

Table XXVII
Weight and Thickness Change of Sintered SiC Sample Tested at the Boiler Condition

Splint Si-SiC - Feed					
Duration (hr)	**PT 1**	**PT 2**	**PT 3**	**Avg. (in)**	**Weight (g)**
0	0.136	0.136		0.1358	6.409
120	0.136	0.136		0.1360	6.409

Splint Si-SiC - Boiler					
Duration (hr)	**PT 1**	**PT 2**	**PT 3**	**Avg. (in)**	**Weight (g)**
0	0.134	0.135		0.1345	6.398
120	0.135	0.135		0.1350	6.394

4.3.20. Fiber Si-SiC

The fiber coupon did not perform as well as the other two Si-SiC composites as dissolution is evident in the coupon after the test (Fig. 43). This is confirmed by the reduction in weight in the specimen (Table XXVIII). It seems some of the matrix materials was dissolved leaving some of the fibers exposed.

Among the three Si-SiC specimens, Bioker 29 and splint, unlike the fiber one, can withstand the corrosiveness of HI_x well. They should be considered as materials for future heat exchanger when the technical difficulties in manufacturing are solved.

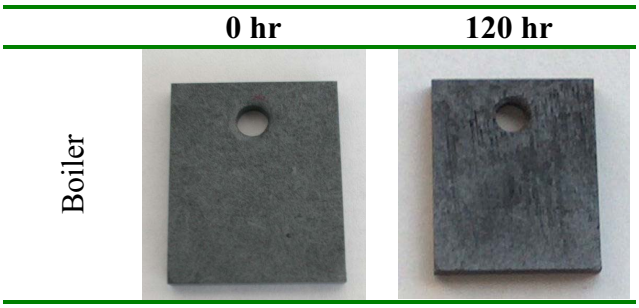

Fig. 43. Fiber Si-SiC coupon tested at the boiler condition for 120 hr.

Table XXVIII
Weight and Thickness Change of Fiber Si-SiC Sample Tested at the Boiler Condition

	Fiber				
Duration (hr)	**PT 1**	**PT 2**	**PT 3**	**Avg. (in)**	**Weight (g)**
0	0.153	0.152	0.1518	0.1524	7.157
120	0.154	0.152	0.153	0.1529	7.113

4.3.21. Alumina (Al_2O_3)

Alumina was tested in HI_x at the feed condition (Fig. 44). There is a measurable weight reduction in the coupon after only 22 hours of test (Table XXIX). Optical examination of the coupon surface revealed small pits (Fig. 45) which points to the fact that Al_2O_3 dissolves in HI_x. This limits the application of Al_2O_3 in HI decomposition.

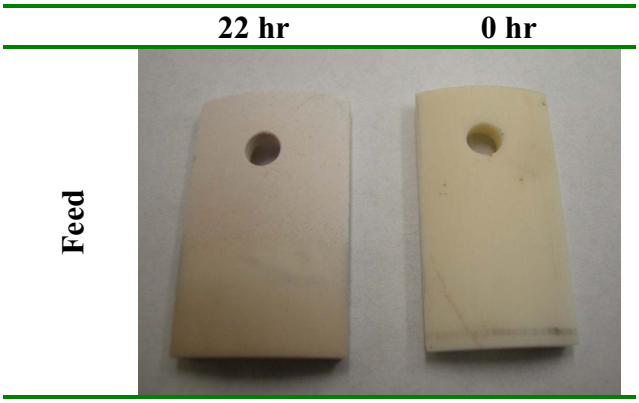

Fig. 44. Alumina coupon tested at the feed condition for 22 hr.

Table XXIX
Weight and Thickness Change of Alumina Coupon Tested at the Boiler Condition

	Alumina				
Duration (hr)	**PT 1**	**PT 2**	**PT 3**	**Avg. (in)**	**Weight (g)**
0	0.119	0.119	0.11915	0.1190	9,868
22	0.120	0.118	0.119	0.1190	9.746

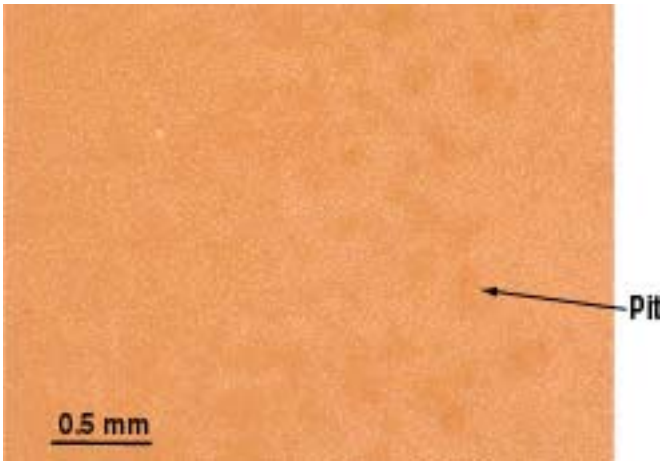

Fig. 45. Alumina coupon showing pits from dissolution in HI_x.

4.3.22. Mullite

Mullite is made from a mixture of Al_2O_3 and SiO_2 and it is very stable by nature. The surface of the test coupon is smooth and shows no sign of corrosion (Fig. 46). The weight loss (Table XXX) in the coupon is due to chipping of the specimen during handling. Hence, even if one can't construct a heat exchanger from mullite, it can be used as containment material.

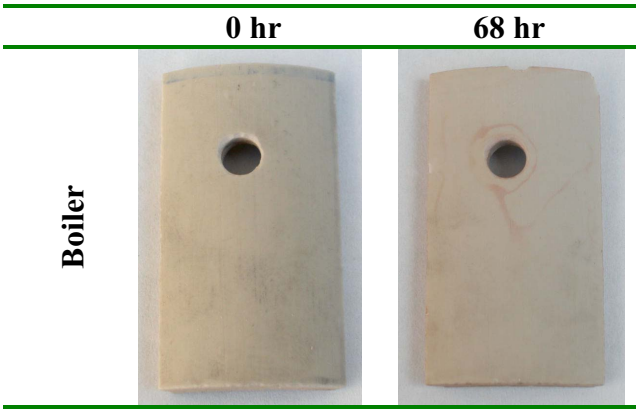

Fig. 46. Mullite coupons (a) new and (b) tested at the boiler condition for a 68 hr.

Table XXX
Weight and Thickness Change of Mullite Tested at the Boiler Condition

	Mullite				
Duration (hr)	**PT 1**	**PT 2**	**PT 3**	**Avg. (in)**	**Weight (g)**
0	0.116	0.117	0.1151	0.1158	7.566
68	0.115	0.116	NA	0.1158	7.503

4.3.23. Graphite

The extruded graphite sample has picked up a significant amount of HI_x during the immersion test (Fig. 47). Its weight has increased by more than 30% as a result of the porosity in the sample (Table XXXI). The sample is structurally sound and there is no evidence of corrosion. Hence, graphite can be used as heat exchanger membrane if the medium on both sides has the similar chemical composition.

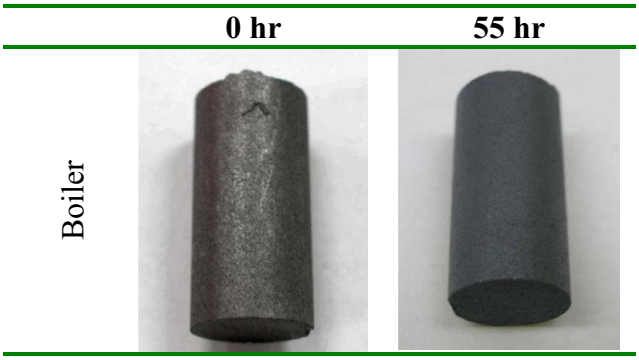

Fig. 47. Extruded graphite rod tested at the boiler condition for 120 hr.

Table XXXI
Weight and Thickness Change of Sintered SiC Sample Tested at the Boiler Condition

	Graphite Rod (1)				
Duration (hr)	**PT 1**	**PT 2**	**PT 3**	**Avg. (in)**	**Weight (g)**
0	0.504	0.504	1.036	0.6813	5.448
120	NA	NA	NA		7.151

4.4. WEIGHT CHANGE AND CORROSION RATE

Tables XXXII and XXXIII show the weight change (normalized by surface area) and the corrosion rate of all the specimens tested for both the feed and boiler conditions. By comparing the general corrosion rate, it is clear that the feed condition is much less corrosive than the boiler condition. The targeted upper corrosion limit for pressurized components is as follow:

Tubing, valves – 0.075mm/yr
Vessel, pipe – 0.5mm/yr

Hence, based on the data obtained at the boiler condition, the materials that satisfy the criteria are:

- Refractory Metals: Ta, Ta-2.5W, Ta-10W Ta-40b, Nb, Nb-10f, Mo-47Re
- Ceramics: Sintered SiC, CVD SiC.

Ta and Nb alloys have better mechanical properties than the pure metals which is important as the system will be pressurized. Hence, development priorities will be placed on Ta-2.5W, Ta-10W and Nb-10Hf. Ta-40Nb is not included because of its limited availability. Other possible candidates include Nb-7.5Ta and Nb-1Zr if an understanding

on the issues encountered during testing can be achieved. Although Mo-47Re satisfies the corrosion criteria, the fact the pure Mo corrodes readily and the high cost of materials makes it an undesirable candidate.

Ceramics materials such as SiC, Si-SiC and even mullite are probable materials but their brittleness and materials characteristics made it difficult to use. In the future, when advances in processing techniques allow the manufacture of monolithic components, then they will be good candidates. In addition, graphite can be a good candidate where permeation is not a concern.

Table XXXII
Weight Change and Corrosion Rate of the Specimens Tested at the Feed Condition

	Material	Condition	Density (g/cc)	Area (cm^2)	Sample Weight Change (mg/cm^2)					Δ weight (g)	Exp. time	Corrosion Rate	
					0 hr	4 hr	20 hr	100 h	120 hr			mpy	mm/yr
1	Alumina	Feed	3.9	22.758	9.868		-5.361			-0.122	22	-215.249	-5.4673
2	SiC (CVD)	Feed	3.21	15.825	6.759				-0.063	-0.001	120	-0.565	-0.0144
3	Ta-10W	Feed	16.9	7.274	30.599				-0.137	-0.001	120	-0.234	-0.0059
4	Nb-1Zr	Feed	8.6	31.032	37.588				-0.064	-0.002	120	-0.215	-0.0055
5	Ta-40Nb	Feed	13.4	28.193	23.026	-0.035	-0.071	-0.035		-0.001	100	-0.091	-0.0023
6	Nb	Feed	8.57	24.114	26.508				0.000	0	1 20	0.000	0.0000
7	Nb-10Hf	Feed	8.9	29.806	28.426				0.000	0	1 20	0.000	0.0000
8	Splint Si-SiC	Feed	2.8	13.391	6.409				0.000	0	1 20	0.000	0.0000
9	Ta	Feed	16.65	24.205	51.137	0.000	0.000	0.041		0.001	100	0.085	0.0022
10	Nb-7.5Ta	Feed	8.7	30.387	34.230	0.000	-0.033	0.099		0.003	100	0.391	0.0099
11	Zircalloy 702	Feed	6.49	31.548	31.262	0.000	0.032	0.095		0.003	100	0.505	0.0128

Alumina was tested for 22 hrs.

Table XXXIII
Weight Change and Corrosion Rate of the Specimens Tested at the Boiler Conditions

					Sample Weight Change (mg/cm^2)									Corrosion Rate	
	Material	Condition	Density (g/cc)	Area (cm^2)	0 hr	4 hr	20 hr	100 hr	120 hr	450 hr	790 hr	Δ weight (g)	Exp. time	mpy	mm/yr
1	Nb-1Zr	Boiler	8.6	31.032	37.302				0.032	-567.217		-17.602	120	-1893.558	-48.0964
2	C-276	Boiler	8.89	28.623	30.854				-335.285			-9.597	120	-1082.779	-27.5026
3	Zircalloy 702	Boiler	6.49	31.548	31.312	-17.497	-17.592					-0.555	20	-466.929	-11.8600
4	Haynes 188	Boiler	8.98	28.882	32.131				-128.833			-3.721	120	-411.888	-10.4620
5	Mo	Boiler	10.3	25.753	29.285				-139.868			-3.602	120	-389.860	-9.9025
6	Bioker 29 Si-SiC	Boiler	2.7	19.320	7.581				-29.400			-0.568	120	-312.616	-7.9404
7	Zircalloy 705	Boiler	6.6	30.323	25.110				-17.479			-0.53	120	-76.032	-1.9312
8	Mullite	Boiler	3.2	20.779	7.566			-3.032				-0.063	68	-48.004	-1.2193
9	Fiber Si-SiC	Boiler	2.8	16.287	7.157				-2.701			-0.044	120	-27.699	-0.7036
10	Nb-7.5Ta	Boiler	8.7	30.387	34.718	-0.066	-0.856	-0.987				-0.03	100	-3.910	-0.0993
11	Splint Si-SiC	Boiler	2.8	12.429	6.398				-0.322			-0.004	120	-3.300	-0.0838
12	SiC (sintered)	Boiler	3.1	39.444	13.318				-0.279			-0.011	120	-2.583	-0.0656
13	Ceramatec SiC (sintered)	Boiler	3.1	35.500	28.954				-0.113			-0.004	120	-1.044	-0.0265
14	Mo-47Re	Boiler	13.52	22.382	6.083				-0.313			-0.007	120	-0.664	-0.0169
15	SiC (CVD)	Boiler	3.21	15.825	7.995				-0.063			-0.001	120	-0.565	-0.0144
16	Ta	Boiler	16.65	24.205	51.010	-0.207	-0.248	-0.248				-0.006	100	-0.513	-0.0130
17	Ta-2.5W -2	Boiler	16.6	26.928	11.277					0.0000		0.000	330	0.000	0.000
18	Ta-2.5W -1	Boiler	16.6	28.279	11.829					0.0354		0.001	330	0.022	0.001
19	Ta-10W	Boiler	16.9	6.378	21.354				-0.157	0.314	0.157	0.001	790	0.040	0.0010
20	Nb-10Hf	Boiler	8.9	29.806	28.181				0.003	0.070	0.104	0.0031	790	0.051	0.0013
21	Ta-40Nb	Boiler	13.4	28.193	23.488	0.071	0.071	0.106				0.003	100	0.274	0.0069
22	Nb	Boiler	8.57	24.114	27.195				0.124			0.003	120	0.417	0.0106
23	Graphite	Boiler	2.2	13.157	5.448				312.590			1.703	120	1689.101	42.9032

- Ta-2.5W coupons were tested for 330 hrs, mullite was tested for 68 hrs.
- Weight reduction in Nb-7.5Ta is mainly due to specimen mishandling (chipping).
- Bioker 29 Si-SiC weight loss is caused by the loss of a corner piece.

5. SUMMARY AND FUTURE WORK

Corrosion coupon immersion tests have been carried out to identify materials of construction candidates for HI decomposition via reactive and extractive distillation. A total of 23 different materials, including refractory metals, reactive metals, superalloys, ceramics and graphite, were tested in HI_x at the reactive column feed and boiler conditions for reactive distillation.

A custom designed high temperature and high-pressure test apparatus was constructed for the experiment. The tests were carried out at high pressure to retard HI_x vapor formation. The design was successful as no corrosion product is observed inside the pressure vessel and system stability is good.

All the metallic specimens tested exhibit color change. This is due to the growth of a passivation layer on the coupons which arises from the reaction between the coupons and HI_x. As this film grows thicker, its color changes correspondingly due to optical effects. The growth rate of this passivation depends primarily on temperature instead of chemical composition. The metal coupons that are corrosion resistant against HI_x all developed an uniform passivation whereas corroded coupons all show uneven color distribution. Table XXXIV is a summary of the corrosion performance of all the materials that have been tested. Metallic materials that perform well include Ta, Nb and their alloys. Sintered and CVD SiC, Bioker 29 and splint Si-SiC composites and mullite are ceramic materials that have excellent corrosion resistance against HI_x.

Severe corrosion has been observed in Zr, Mo, Ni-based and Co-based superalloys. Corrosion is manifested as both pitting and dissolution and is not evenly spread on the coupon. This may have been caused by chemical gradient in the HI_x medium. Unexpected corrosion has been observed in Nb-1Zr coupon but it could possibly be a result of contamination.

Based on test results and materials availability, three alloys, Ta-2.5W, Ta-10W and Nb-10Hf, are selected for developmental testing. They will undergo long term immersion testing for up to 1000hrs or until the surface passivation is stable and no longer changes color. The effect of processing on the corrosion performance of these materials will be investigated.

Table XXXIV
Summary of the Immersion Coupon Corrosion Screening Test Results

	Materials	Boiler	Feed
1	Ta	Good	Good
2	Ta-2.5W	-	Excellent
3	Ta-10W	Excellent	Excellent
4	Ta-40Nb	Excellent	Excellent
5	Nb	Good	-
6	Nb-1Zr	Excellent	Good
7	Nb-7.5Ta	Fair	Good
8	Nb-10Hf (C103)	Excellent	Excellent
9	Mo	Poor	-
10	Mo-47Re	Fair	-
11	Zircalloy 702	Poor	Poor
12	Zircalloy 705	Poor	-
13	C-276	Poor	-
14	Haynes 188	Poor	-
15	SiC (sintered)	Good	-
16	Ceramatec SiC (sintered)	Excellent	-
17	SiC (CVD)	Excellent	Excellent
18	Bioker 29 Si-SiC	Good	-
19	Splint Si-SiC	Good	Good
20	Fiber Si-SiC	Good	-
21	Alumina	-	Fair
22	Mullite	Excellent	-
23	Graphite	Poor*	-

Excellent: very minor change in color due to passivation
Good: distinguish color change due to passivation
Fair: mild corrosion- localized oxidation, uneven passivation and minor weight loss
Poor: severe corrosion - dissolution and pitting

6. REFERENCES

[1] L.C. Brown, G.E. Besenbruch, R.D. Lentsch, K.R. Schultz, J.F. Funk, P.S. Pickard, A.C. Marshall, K.S. Showalter, "High Efficiency Generation of Hydrogen Fuels Using Nuclear Power," General Atomics Report GA-A24285 Rev. 1 (2003).

[2] M. Roth and K.F. Knoche, J. Hydrogen Energy **14**, 545 (1989).

[3] J.H. Norman, G.E. Besenbruch and D.R. O'Keefe, "Therochemical Water-Splitting for Hydrogen Production," General Atomics Report GA-A16300 (Gas Research Institute Report 80/0105) March 1981.

[4] L.C. Brown, R. Buckingham, G.E. Besenbruch, B. Wong, G. Polansky and P.S. Pickard, "Engineering Materials Requirements Assessment for the S-I Thermochemical Cycle," General Atomics Report GA-A24902 (2004).

[5] P.W. Trester and H G. Staley, Gas Research Institute Report 80/00981, May (1981).

[6] Z.M. Shappiro, *Metallurgy of Ziroconium*, Eds. B. Lustman and F. Kerze Jr., McGraw Hill, New York (1955) pg. 135.

[7] Internal test data, Wah Chang Inc.

[8] Handbook of Corrosion Data, ASM International (1990) p. 412.

[9] A. Robin, J.L. Rosa, "Corrosion Behavior of Niobium, Tantalum and Their Alloys in Hot Hydrochloric and Phosphoric Acid Solutions," Int Journal of Refractory Metals and Hard Materials **18**, 13 (2000) 13-21.

[10] F.H. Gern and R. Kochendoerfer, "Liquid Silicon Infiltration: Description of Iinfiltration Dynamics and Silicon Carbide Formation," Composite Part A **28A**, 355 (1997).

[11] P.F. Peterson, C.W. Forsberg and P.S. Pickard, "Advanced CSiC Composites for High-Temperature Nuclear Heat Transport with Helium, Molten Salts and Sulfur-Iodine Thermomechanical Hydrogen Process Fluids," 2nd Information Exchange Meeting on Nuclear Production of Hydrogen, Argonne National Laboratory, Illinois (2003).

Other related reference (HI)

"Study on HIx Cycling Techniques for Thermo Chemical Hydrogen Production Process (R & D on Refractory and Corrosion Resistant Pressure Sensor for Hydrogen Iodide Cycling Test Loop)". Ishiyama, Shintaro, Nippon Kikai Gakkai Ronbunshu A **69**, 1510 (2003.

P.W. Trester, S.S. Liang, "Material Corrosion Investigations for the General Atomic Sulfur-Iodine Thermochemical Water-Splitting Cycle Hydrogen Energy System," Proceedings of the Second World Hydrogen Energy Conf., Zurich, Switzerland, (1978). Pergamon Press, Vol. 4. (1979) pg. 2113-2159.

Y. Imai, Y. Kanda, H. Sasaki, H. Togano, "Corrosion Resistance of Metallic Materials in High Temperature Gases Composed of Iodine, Hydrogen Iodide and Water (Environment of the 3rd and 4th Stage Reactions) (Retroactive Coverage)," Boshoku Gijutsu (Corros. Eng.) Vol. 31 (1982) p. 714.

W. Kondo, M. Kaneko, Y. Takemori, H. Sasaki, "Corrosion Resistance of Ceramic Materials in High Temperature Gases Composed of Iodine, Hydrogen Iodide and Water (Environment of the 3rd and 4th State Reactions) (Retroactive Coverage)," Boshoku Gijutsu (Corros. Eng.) Vol. 31 (1982) p. 722.

H. Sasaki, Y. Kanda, Y. Imai, H. Togano, "Corrosion Resistance of Materials in Concentrated Solutions of Iodine and Iodide (Environment of the 1st Stage Reaction) (Retroactive Coverage)," Boshoku Gijutsu (Corros. Eng.) Vol. 31 (1982) p . 691.

Iodine

Y. Imai, "Corrosion Study of Equipment Materials for Magnesium-Iodine Thermochemical Hydrogen Production Process and Protective Coating by Plasma CVD," J. Natl. Chem. Lab. Ind. (Japan) **87**, 1 (1992).

I. Schuster, C. Lemaignan, "Characterisation of Zircaloy Corrosion Fatigue Phenomena in an Iodine Environment. I. Crack Growth. (Retroactive Coverage)," J. Nucl. Mater. **166**, 348 (1989).

P.S. Sidky, "Iodine Stress Corrosion Cracking of Zircaloy Reactor Cladding: Iodine Chemistry (A Review)," J. Nucl. Mater. (Netherlands) **256**, 1 (1998).

S.K. Ghosal, P.K. De, "Stress Corrosion Cracking of Zircaloys in Halogen Containing Environments," Proceedings of the Symposium Zirconium (2002).

S. Shann, D.R.. Olander, "Correlation of Failure Times for Iodine Stress Corrosion Cracking of Zircaloy," Nucl. Technol. **53**, 407 (1981).

J.C. Wren, G.A. Glowa, J. Merritt, "Corrosion of Stainless Steel by Gaseous I_2," J. Nucl. Mater. **265**, 161(1999).

S.B. Farina, G.S. Duffo, J.R. Galvele, "Stress Corrosion Cracking of Zirconium and Zircaloy-4 in Iodine Containing Solutions," Corrosion (2002).

S.K. Ghosal, P.K. De, "Texture, Temperature and Iodine Effects on Stress Corrosion Cracking of Zircaloy-2," Int. Conf. on Advances in Materials Processing (ICAMMP-2002) p. 139.

I. Schuster, C. Lemaignan, "Characterisation of Zircaloy Corrosion Fatigue Phenomena in an Iodine Environment. II. Fatigue Life. (Retroactive Coverage)," J. Nucl. Mater. **166**, 357 (1989).

ACKNOWLEDGMENT

This work was funded by the U.S. Department of Energy through the University of Nevada Las Vegas Research Foundation Subcontract #RF-05-HTHX-005.